Generation of the Highly Reactive Intermediates $Cp^*_2Zr{=}O$ and $Cp^*_2Zr{=}S$: Trapping Reactions with Alkynes, Nitriles, and Dative Ligands

Michael J. Carney, Patrick J. Walsh, Frederick J. Hollander, and Robert G. Bergman*

Department of Chemistry, University of California, Berkeley, California 94720

Received October 9, 1991

This paper outlines synthetic procedures that result in the successful generation of the long-sought oxo complex [$Cp^*_2Zr{=}O$] and its sulfur analogue [$Cp^*_2Zr{=}S$]. The generation of [$Cp^*_2Zr{=}O$] has been accomplished at 160 °C by α-elimination of benzene from $Cp^*_2Zr(Ph)(OH)$ (**1**) and at room temperature by deprotonation of $Cp^*_2Zr(OH)(OSO_2CF_3)$ with $KN(SiMe_3)_2$. The oxo species reacts with diphenylacetylene and di-*p*-tolylacetylene to give oxametallacyclobutenes $Cp^*_2Zr(OC(Ph){=}C(Ph))$ (**5a**) and (Cp^*_2Zr(OC-(Tol)=C(Tol)) (**5b**), which are stable at room temperature. At the elevated temperatures necessary for the α-elimination of benzene from **1**, however, these complexes rearrange to ortho-metalated oxametallacycles $Cp^*_2Zr(OC(o\text{-}C_6H_4){=}C(Ph)(H))$ (**2a**) and $Cp^*_2Zr(OC(o\text{-}C_6H_4CH_3){=}C(Tol)(H))$ (**2b**), and these are the products isolated in the 160 °C thermolysis of **1**. Similarly, generation of [$Cp^*_2Zr{=}O$] at 160 °C in the presence of 1,4-diphenyl-1,3-butadiyne yields the complex metallacycle $(\eta^5\text{-}C_5(CH_3)_5)Zr(OC(Ph){=}C(H)$-$=C(Ph)(\eta^5\text{-}C_5(CH_3)_4CH_2))$ (**3**), in which one Cp* ligand has been integrated into the coordinated enolate moiety. In the presence of excess benzonitrile at both high and low temperature the oxo complex yields the six-membered oxaazametallacycle $Cp^*_2Zr(OC(Ph){=}NC(Ph){=}N)$ (**4a**), formed from insertion of 2 equiv of PhCN into the Zr=O fragment. The connectivities of complexes **2a**, **3**, and **4a** were confirmed by X-ray structure determinations. At room temperature, reaction of [$Cp^*_2Zr{=}O$] with the unsymmetrical alkyne 1-phenyl-1-propyne proceeds regiospecifically, yielding only the metallacycle $Cp^*_2Zr(OC(Me){=}C(Ph))$ (**5d**), having the phenyl substituent located α to the metal center; this material gives phenylacetone upon hydrolysis. Kinetic, alkyne-exchange, and isotope-labeling studies support a mechanism involving direct elimination of benzene from **1** in the thermal generation of [$Cp^*_2Zr{=}O$]. They also suggest that the rearrangement of the oxametallacyclobutenes **5a,b** may proceed by initial reversion of the metallacycle to an oxo–alkyne complex followed by attack of oxygen on the phenyl ring of the alkyne. The isoelectronic sulfido complex [$Cp^*_2Zr{=}S$] is generated by room temperature dehydrohalogenation of $Cp^*_2Zr(SH)(I)$ (**10**). In analogy to the earlier generated imido complexes [$Cp_2Zr{=}N{-}R$], the sulfido complex can be stabilized and isolated in pure form as the dative ligand adduct [$Cp^*_2(L)Zr{=}S$] (L = pyridine (**11a**), 4-*tert*-butylpyridine (**11b**)). An X-ray structure determination of **11b** confirmed the unusual Zr=S bonding mode and represents the first example of this structural type among group 4 metals. Like its oxo analogue, the Zr=S multiply bonded linkage reacts with nitriles and alkynes to form the thiaazametallacycle $Cp^*_2Zr(SC(Ph){=}NC(Ph){=}N)$ (**12**) and the thiametallacyclobutenes $Cp^*_2Zr(SC(R){=}C(R))$ (**13a–c**, R = Et, Ph, Tol). The latter structural type was confirmed by an X-ray structure determination of **13b**. The thiametallacyclobutenes readily revert to the monomeric terminal sulfido complexes **11** and free alkyne by reaction of the metallacyclobutene with pyridine; with appropriate alkynes and dative ligands, equilibria between the thiametallacyclobutenes and ligand-trapped sulfido complexes can be established and directly observed by NMR spectrometry in solution. Judging from these observations, the sulfido ligand appears to be the most stable linkage in the Zr=X (X = NR, O, S) series.

Introduction

Many mononuclear transition-metal complexes that contain multiple bonds between metals and heteroatoms such as oxygen and nitrogen are known, and a few of the corresponding M=S complexes have also been prepared. Although there are several complexes with M=O bonds (e.g., permanganate, ruthenate) that can be used to effect overall oxidation of organic compounds, only rarely have reactions that produce direct adducts between M=X bonds and organic molecules been identified and studied in depth.[1,2] In principle, new M=X (X = NR, O, S) linkages capable of reacting with unsaturated organic compounds could be useful in the development of new organic functionalization reactions (i.e. in the formation of new carbon–heteroatom bonds). Examples of this type of reactivity found in biological and biomimetic systems include the conversion of alkenes to epoxides using cytochrome P450 and related model systems.[3a] Examples from synthetic chemistry that underscore the potential utility of metal-mediated heteroatom-transfer reactions include catalyzed alkene oxidations (some of which can be carried out with high levels of asymmetric induction) mediated by ruthenium, titanium, rhodium, and osmium[3b,c] complexes.

It was recently discovered in these laboratories[4] that α-elimination of methane from $Cp_2Zr(Me)(NH\text{-}t\text{-}Bu)$ (Cp = $\eta^5\text{-}C_5H_5$) generates the transient species [$Cp_2Zr{=}N\text{-}t$-Bu]. Some of the chemistry of this intermediate is illustrated in Scheme I. In contrast to the vast majority of other metal–imido complexes, this intermediate is extraordinarily reactive toward organic compounds and undergoes cycloaddition reactions with alkynes (often regiospecifically) to give azametallacyclobutenes.[5] Other

(1) (a) Nugent, W. A.; Mayer, J. A. *Metal-Ligand Multiple Bonds*; Wiley-Interscience: New York, 1988. (b) Holm, R. H. *Chem. Rev.* **1987**, *87*, 1401 and references therein.

(2) The few known examples include reactions of certain Cp*Re oxo complexes (Herrmann, W. A. *J. Organomet. Chem.* **1986**, *300*, 111) and the recently reported $Cp^*_2W{=}O$ (Parkin, G.; Bercaw, J. E. *J. Am. Chem. Soc.* **1989**, *111*, 391).

(3) (a) Ortiz de Montellano, P. R. *Cytochrome P450*; Plenum Press: New York, 1986. (b) Jacobsen, E. N.; Markó, I. E.; Mungall, W. S.; Schröder, G. W.; Sharpless, K. B. *J. Am. Chem. Soc.* **1988**, *110*, 1968. (c) Wai, J. S. M.; Markó, I. E.; Svendsen, J. S.; Finn, M. G.; Jacobsen, E. N.; Sharpless, K. B. *J. Am. Chem. Soc.* **1989**, *111*, 1123.

(4) Walsh, P. J.; Hollander, F. J.; Bergman, R. G. *J. Am. Chem. Soc.* **1988**, *110*, 8729.

0276-7333/92/2311-0761$03.00/0

Scheme I

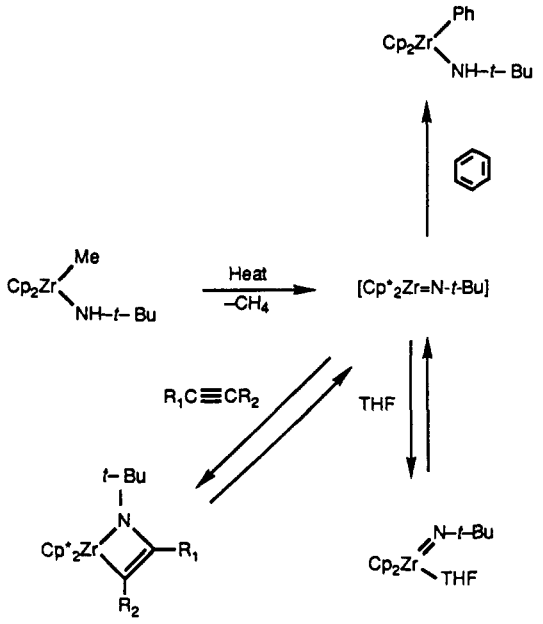

reactions of $[Cp_2Zr{=}N\text{-}t\text{-}Bu]$[4] shown in Scheme I include C–H activation of benzene to generate $Cp_2Zr(Ph)(NH\text{-}t\text{-}Bu)$ and trapping with THF and other dative ligands to form monomeric terminal imido compounds.

These results prompted us to examine whether the isoelectronic Zr=O and Zr=S species might be generated from complexes of general structure $Cp_2Zr(R)(XH)$ (R = alkyl, aryl; X = O, S) by a process similar to the α-elimination reaction shown in Scheme I. However, until very recently we were unable to find examples of monomeric complexes in the literature appropriate for investigating as starting materials. Presumably such complexes are unstable with respect to dimerization through the X atom, as there are many examples of heteroatom-bridged zirconium dimers.[6] It seemed likely that the more sterically demanding Cp* ligand (Cp* = η^5-C_5Me_5) might inhibit this dimerization. Our attempt to test this possibility was stimulated by reports describing $Cp^*_2Zr(Ph)(OH)$[7] and $Cp^*_2Zr(Cl)(OH)$,[8] and we have subsequently prepared the analogous sulfur complex $Cp^*_2Zr(I)(SH)$ (vide infra). In this paper we wish to report the successful use of these precursors to generate $[Cp^*_2Zr{=}O]$ and $[Cp^*_2Zr{=}S]$, the subsequent reactivity of these unsaturated species with organic compounds and dative ligands, and some unusual rearrangement reactions of these trapped products.[9]

Results and Discussion

Thermolysis of $Cp^*_2Zr(Ph)(OH)$ (1) in the Presence of Alkynes and Nitriles. With the goal of mimicking the successful generation of $[Cp_2Zr{=}NR]$, we attempted a similar α-elimination reaction by heating $Cp^*_2Zr(Ph)(OH)$ (1), recently prepared by Marks,[7a] in the presence of alkynes. Our hope was that benzene would be eliminated to form $[Cp^*_2Zr{=}O]$, which could be trapped to give oxazirconacyclobutenes or dative-ligand complexes analogous to $Cp_2(THF)Zr{=}NR$. Thermolysis of 1 in the presence of dative ligands such as triphenylphosphine oxide or various substituted pyridines in sealed NMR tubes did result in the slow disappearance of 1 with the concomitant appearance of benzene (as judged by ^1H NMR spectrometry). Unfortunately, the high temperature necessary to effect elimination of benzene from 1 (130–160 °C) resulted in the formation of a multitude of Cp*-containing species. Similarly, heating 1 at 160 °C in the presence of excesses of alkynes such as 3-hexyne, 2-butyne, and 1-phenyl-1-propyne did not yield tractable products.

Scheme II

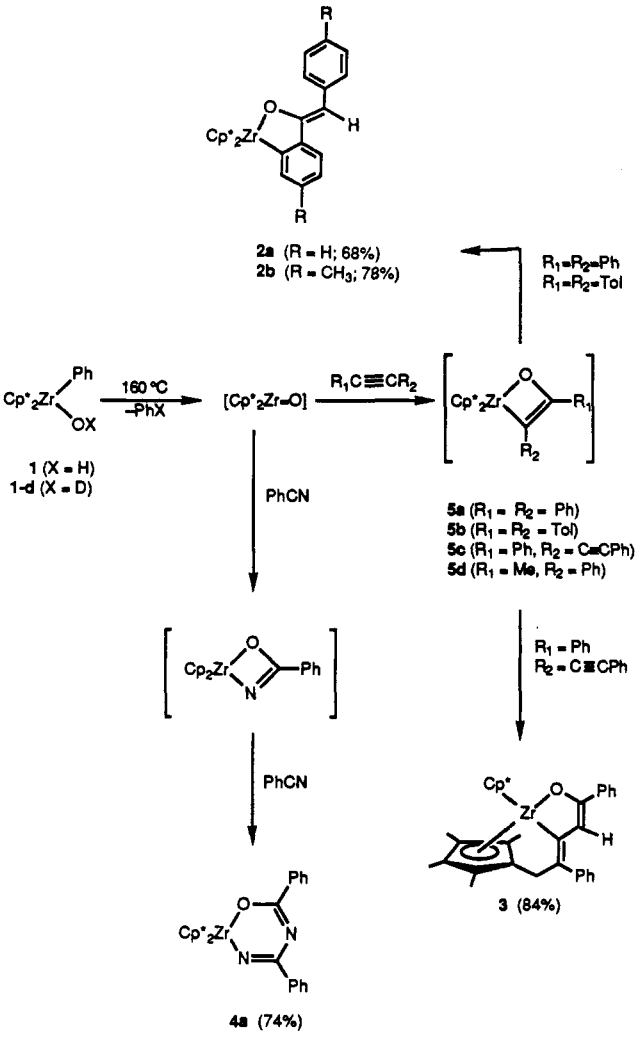

However, as shown in Scheme II, thermolysis of 1 at 160 °C (benzene, Pyrex bomb) in the presence of 3–4 equiv of diphenylacetylene did yield a single product, formulated as the ortho-metalated oxametallacycle **2a**, in 68% isolated yield (92% by ^1H NMR spectrometry). A vinylic hydrogen resonance (6.27 ppm) and the phenyl region pattern in the ^1H NMR spectrum (C_6D_6), as well as a resonance at 196 ppm in the ^{13}C NMR spectrum characteristic of an sp^2 carbon bound to zirconium(IV),[10] are suggestive of the ortho-metalated structure. This assignment was confirmed by an X-ray crystal structure determination of **2a**. Suitable

(5) For other recent examples of reactive metal–imido complexes, see: (a) Cummins, C. C.; Baxter, S. M.; Wolczanski, P. T. *J. Am. Chem. Soc.* **1988**, *110*, 8731. (b) Cummins, C. C.; Schaller, C. P.; Van Duyne, G. D.; Wolczanski, P. T.; Chan, A. W. E.; Hoffmann, R. *J. Am. Chem. Soc.* **1991**, *113*, 2985. (c) Glueck, D. S.; Hollander, F. J.; Bergman, R. G. *J. Am. Chem. Soc.* **1989**, *111*, 2719.

(6) For example, see: Hunter, W. E.; Hrncir, D. C.; Vann Bynum, R.; Penttila, R. A.; Atwood, J. L. *Organometallics* **1983**, *2*, 750.

(7) (a) Schock, L. E.; Marks, T. J. *J. Am. Chem. Soc.* **1988**, *110*, 7701. (b) Schock, L. E.; Brock, C. P.; Marks, T. J. *Organometallics* **1987**, *6*, 232.

(8) Bortolin, R.; Patel, V.; Munday, I.; Taylor, N. J.; Carty, A. J. *J. Chem. Soc., Chem. Commun.* **1985**, 456.

(9) Preliminary accounts of this work have appeared: (a) Carney, M. J.; Walsh, P. J.; Hollander, F. J.; Bergman, R. G. *J. Am. Chem. Soc.* **1989**, *111*, 8751. (b) Carney, M. J.; Walsh, P. J.; Bergman, R. G. *J. Am. Chem. Soc.* **1990**, *112*, 6426.

(10) For example, the ^{13}C resonance corresponding to the sp^2 carbon atoms bound to Zr in $Cp^*_2ZrPh_2$ appear at 193.47 ppm (C_6D_6).[7b]

Table I. Summary of Crystal and Data Collection Parameters[a]

	2a	3	4a	11b	13b
formula	$C_{34}H_{40}OZr$	$C_{36}H_{40}OZr$	$C_{34}H_{40}N_2OZr \cdot {}^1/_2C_7H_8$	$C_{29}H_{44}NSZr$	$C_{34}H_{40}SZr$
fw	555.91	579.93	630.00	528.96	571.98
a, Å	9.4243 (10)	9.6706 (17)	9.4840 (20)	9.7531 (28)	17.143 (4)
b, Å	18.7513 (17)	10.2703 (11)	17.5041 (19)	14.8294 (22)	12.566 (2)
c, Å	16.8210 (17)	30.132 (1)	20.670 (1)	19.4382 (38)	13.421 (3)
α, deg	90.0	90.0	90.0	90.0	90.0
β, deg	101.882 (9)	96.285 (12)	103.960 (15)	90.876 (28)	90.0
γ, deg	90.0	90.0	90.0	90.0	90.0
V, Å^3	2908.9 (9)	2974.8 (1.2)	3330.1 (1.7)	2811 (2)	2891.2 (2.1)
Z	4	4	4	4	4
space group	$P2_1/n$	$P2_1/n$	$P2_1/c$	$P2_1/c$	$Pna2_1$
T, K	298	298	298	191	191
λ, Å	0.71073	0.71073	0.71073	0.71073	0.71073
d_{calc}, g cm^{-3}	1.27	1.30	1.26	1.25	1.31
μ, cm^{-1}	3.9	3.8	3.5	4.7	4.6

[a] Further details are given in the supplementary material provided with ref 9.

Table II. Selected Interatomic Distances[a] (Å) for Complexes 2a, 3, 4a, 11b, and 13b

	Compound **2a**		
Zr–O	2.028 (1)	O–C27	1.349 (2)
Zr–C21	2.276 (2)	C21–C26	1.414 (3)
Zr–Cp1	2.235	C26–C27	1.482 (3)
Zr–Cp2	2.250	C27–C28	1.357 (3)
Zr–C21	2.276 (2)		
	Compound **3**		
Zr–O	2.059 (1)	C22–C21	1.362 (3)
Zr–C22	2.253 (2)	C21–C20	1.530 (3)
O–C24	1.356 (2)	C21–C31	1.472 (3)
C21–C22	1.362 (3)	C24–C25	1.480 (3)
C24–C23	1.355 (3)	Zr–Cp1	2.253
C23–C22	1.455 (3)	Zr–Cp2	2.207
C23–C24	1.355 (3)	C15–C20	1.496 (3)
	Compound **4a**		
Zr–ON1	2.063 (1)	C8–ON2	1.285 (3)
Zr–ON2	2.060 (2)	C1–N1	1.357 (3)
Zr–Cp1	2.244	C8–N1	1.357 (3)
Zr–Cp2	2.249	C1–C2	1.505 (3)
C1–ON1	1.285 (3)		
	Compound **11b**		
Zr–S	2.316 (1)	Zr–Cp2	2.298 (4)
Zr–N	2.341 (4)	N–C1	1.346 (6)
Zr–Cp1	2.296 (4)	N–C5	1.342 (6)
	Compound **13b**		
Zr–S	2.505 (1)	C1–C2	1.510 (6)
Zr–C8	2.226 (4)	C1–C8	1.330 (6)
S–C1	1.829 (5)	C8–C9	1.488 (6)

[a] Full interatomic distance data are provided as supplementary material in ref 9. Metal–Cp distances refer to Cp centroids.

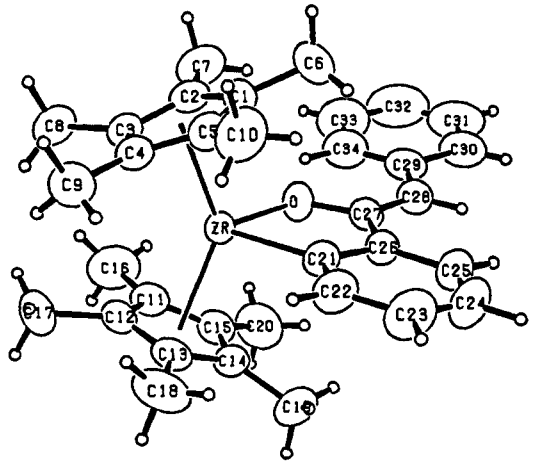

Figure 1. ORTEP diagram of diphenylacetylene addition product **2a** with 50% probability thermal ellipsoids. The diagram shows the numbering scheme used in the tables.

Table III. Selected Bond Angles[a] (deg) for Complexes 2a, 3, 4a, 11b, and 13b

	Compound **2a**		
O–Zr–C21	75.54 (6)	Zr–C21–C22	132.2 (2)
O–Zr–Cp1	105.86	Zr–C21–C26	110.66 (14)
O–Zr–Cp2	107.87	C21–C26–C27	116.7 (2)
C21–Zr–Cp1	105.96	C26–C27–O	112.9 (2)
C21–Zr–Cp2	103.96	C28–C27–O	122.3 (2)
Cp1–Zr–Cp2	139.31	C26–C27–C28	124.7 (2)
Zr–O–C27	123.89 (12)	C27–C28–C29	129.7 (2)
	Compound **3**		
Cp1–Zr–O	109.00	C22–C21–C31	126.89 (18)
Cp2–Zr–O	110.53	Zr–C22–C21	124.33 (14)
Cp1–Zr–C22	105.99	Zr–C22–C23	106.00 (12)
Cp2–Zr–C22	94.17	C21–C22–C23	128.64 (18)
Cp1–Zr–Cp2	138.87	C22–C23–C24	115.07 (18)
O–Zr–C22	75.97 (6)	O–C24–C23	119.18 (17)
C15–C20–C21	110.34 (17)	O–C24–C25	114.96 (18)
C20–C21–C22	115.33 (18)	C23–C24–C25	125.79 (19)
C20–C21–C31	117.60 (17)	Zr–O–C24	114.70 (12)
	Compound **4a**		
Cp1–Zr–ON1	104.79 (4)	ON1–C1–N1	127.8 (2)
Cp2–Zr–ON1	105.71 (4)	ON2–C8–N1	127.2 (2)
Cp1–Zr–ON2	105.02 (5)	C1–N1–C8	120.9 (2)
Cp2–Zr–ON2	104.20 (4)	ON1–C1–C2	118.1 (2)
Cp1–Zr–Cp2	139.88 (1)	N1–C1–C2	114.1 (2)
ON1–Zr–ON2	82.60 (6)	ON2–C8–N1	127.2 (2)
Zr–ON1–C1	130.25 (14)	ON2–C8–C9	117.8 (2)
Zr–ON2–C8	130.87 (14)	N1–C8–C9	115.0 (2)
	Compound **11b**		
S–Zr–N	91.85 (9)	C1–N–C5	116.1 (4)
Zr–N–C1	122.6 (3)	Cp1–Zr–Cp2	136.4 (4)
Zr–N–C5	120.5 (3)		
	Compound **13b**		
S–Zr–C8	70.86 (11)	C2–C1–C8	127.8 (4)
Zr–S–C1	74.22 (15)	Zr–C8–C1	93.9 (3)
S–C1–C2	111.8 (3)	Zr–C8–C9	140.7 (3)
S–C1–C8	120.3 (3)	C1–C8–C9	125.0 (4)

[a] Full interatomic angle data are provided as supplementary material in ref 9.

yellow-orange blocklike crystals were grown by diffusing hexane into a saturated benzene solution of **2a** and exist in the space group $P2_1/n$. The structure was solved by Patterson methods and refined by standard least-squares and Fourier techniques. Crystal and data collection parameters are included in Table I. An ORTEP diagram is shown in Figure 1, and selected bond distances and angles are provided in Tables II and III, respectively.[11] The zirconium atom is coordinated in a standard pseudotet-

(11) Other data are given in supplementary material supplied with the preliminary communications.[9]

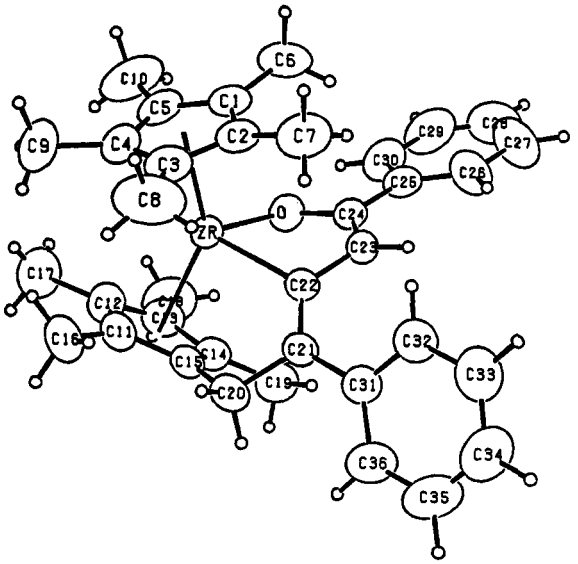

Figure 2. ORTEP diagram of 1,4-diphenyl-1,3-butadiyne insertion product **3** with 50% probability thermal ellipsoids. The diagram shows the numbering scheme used in the tables.

rahedral fashion by the two Cp* ligands, the oxygen atom, and an ortho carbon of one phenyl ring. The five-membered metallacycle is planar to ±0.04 Å; in fact, the entire coordinated enolate functionality is nearly planar, with only small twists of the ortho-metalated and free phenyl rings (5 and 4°, respectively) with respect to the metallacycle plane. The Zr–O (2.028 (1) Å) and Zr–C21 (2.276 (2) Å) distances are typical of single bonds between zirconium(IV) and these atom types.[12] The distances C27–O (1.349 Å) and C27–C28 (1.357 Å) are respectively slightly shorter and longer than might be expected for localized C—O and C=C single and double bonds, suggestive of some delocalization through the five-membered ring.

Thermolysis of **1** in the presence of excess di-*p*-tolylacetylene (Scheme II) yields the corresponding di-*p*-tolyl ortho-metalated compound **2b** in 78% isolated yield after removal of excess alkyne by sublimation of the alkyne onto a cold finger. The presence of a vinylic hydrogen (6.24 ppm) and two *p*-tolyl methyl group (2.34, 2.28 ppm) resonances in the ^{1}H NMR spectrum (C_6D_6) as well as the characteristic metalated sp^2 carbon signal (195.4 ppm) in the ^{13}C NMR spectrum confirmed the structure of **2b** by analogy to that of **2a**. The formation of **2b** clearly indicates that the phenyl group originally bound to Zr in **1** is liberated during thermolysis. This point will be addressed in more detail later.

Heating **1** (160 °C, benzene solvent, Pyrex bomb) in the presence of 3–4 equiv of 1,4-diphenyl-1,3-butadiyne yields a deep red compound (**3**, 84% yield) which possesses a ^{1}H NMR spectral pattern similar to that of a (η^5-C_5Me_5)(η^5:η^1-$C_5Me_4CH_2$)ZrX "cyclometalated" species. However, the CH_2 protons in such cyclometalated compounds typically appear as diastereotopic doublets near 2 ppm[13] (Zr directly bound to CH_2), whereas the resonances in **3** appear further downfield at 3.5 and 3.8 ppm (^{1}H NMR, THF-d_8). Also, the ^{13}C resonance attributable to the methylene carbon in cyclometalated compounds is normally found between 60 and 70 ppm;[14] the methylene

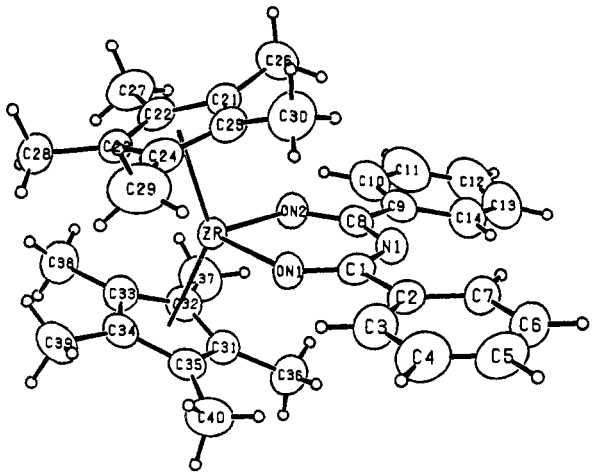

Figure 3. ORTEP diagram of benzonitrile addition product **4a** with 50% probability thermal ellipsoids. The diagram shows the numbering scheme used in the tables.

carbon in **3** appears at 34.6 ppm (C_6D_6). These NMR results suggest that the methylene carbon is probably not directly bound to zirconium and are more in accord with the structure for **3** shown in Scheme II. An X-ray structure determination confirmed this unique bonding arrangement. Suitable crystals were obtained by diffusion of hexane into a THF solution of **3**. The structure was solved by Patterson methods and refined by standard least-squares and Fourier techniques. Crystal (space group $P2_1/n$) and data collection parameters are included in Table I. An ORTEP diagram is shown in Figure 2, and selected bond distances and angles are provided in Tables II and III, respectively. The structure is characterized by discrete molecules with no unusually close intermolecular contacts. The zirconium atom is coordinated in the standard η^5 manner to one Cp* ligand, with the remaining three coordination sites being occupied by the unusual Cp*–enolate functionality. The Zr–O (2.059 (1) Å) and Zr–C22 (2.253 (2) Å) distances are once again typical of Zr(IV)–O and Zr(IV)–C(sp^2) bond lengths. In addition, the C21–C22 (1.362 (3) Å) and C23–C24 (1.355 (3) Å) distances are within the range found for C=C double bonds and much shorter than C22–C23 (1.455 (3) Å), indicating localization in the metallacycle. The distance from the Zr atom to the Cp* ligand bonded to the enolate is significantly shorter than the other Zr–Cp* distance (2.207 vs 2.253 Å), due to ring strain in the Cp*–enolate ligand.

In an attempt to trap the presumed [Cp^*_2Zr=O] intermediate, we examined the thermolysis of **1** in the presence of 4 equiv of benzonitrile. However, this reaction consumed 2 equiv of PhCN/mol of **1**, affording an orange-yellow compound formulated as the six-membered metallacycle **4a** in 74% isolated yield after recrystallization from ether (Scheme II). The ^{1}H and ^{13}C NMR spectra of this compound are consistent with the presence of two inequivalent, freely rotating phenyl rings. Once again, an X-ray structure analysis confirmed the proposed connectivity. Single crystals were obtained by layering hexane on a saturated toluene solution of **4a**. This yielded crystals with one molecule of toluene in the cell for every two molecules of **4a**. Crystal and X-ray collection data are given in Table I, and an ORTEP diagram is shown in Figure 3; selected bond distances and angles are provided in Tables II and III, respectively. Due to the high pseudosymmetry of the metallacycle (see Scheme II and Figure

(12) The Zr to phenyl carbon distance in (η^5-C_5Me_5)(η^5:η^1-$C_5Me_4CH_2$)ZrPh is 2.285 Å.[7b] The Zr–O and Zr–C(sp^2) distances in the Cp^*_2Zr(*s-cis*-isoprene)–diphenylketene (1:1) adduct are 2.000 and 2.236 Å, respectively (Yasuda, H.; Okamoto, T.; Matsuoka, Y.; Nakamura, A.; Kai, Y.; Kanehisa, N.; Kasai, N. *Organometallics* **1989**, *8*, 1139).

(13) For example, the cyclometalated methylene protons in (η^5-C_5Me_5)(η^5:η^1-$C_5Me_4CH_2$)ZrPh appear at 2.24 and 2.07 ppm (C_6D_6).[7b]

(14) The corresponding CH_2 ^{13}C resonance in (η^5-C_5Me_5)(η^5:η^1-$C_5Me_4CH_2$)ZrPh occurs at 63.5 ppm (C_6D_6).[7b]

Table IV. Rate Constants for the Thermolysis of 1 at 160 °C

compd	trapping ligand	amt. of trap added, equiv	solvent	k_{obs}, 10^5 s^{-1}
1	di-*p*-tolylacetylene	3.3	C_6D_6	3.64
1	di-*p*-tolylacetylene	3.5	C_6D_6	3.23
1	di-*p*-tolylacetylene	7.0	C_6D_6	3.24
1	di-*p*-tolylacetylene	11.5	C_6D_6	3.20
1	di-*p*-tolylacetylene	5.5	C_6D_6[a]	3.61
1	di-*p*-tolylacetylene	4.0	THF-d_8	3.57
1	1,4-diphenyl-1,3-butadiyne	5.6	C_6D_6	3.55
1	1,4-diphenyl-1,3-butadiyne	9.8	C_6D_6	3.57
1	benzonitrile	6.6	C_6D_6	3.63
1-*d*	di-*p*-tolylacetylene	3.0	C_6D_6	0.77
1-*d*	di-*p*-tolylacetylene	4.3	C_6D_6	0.80

[a] 1 equiv of pyridine added.

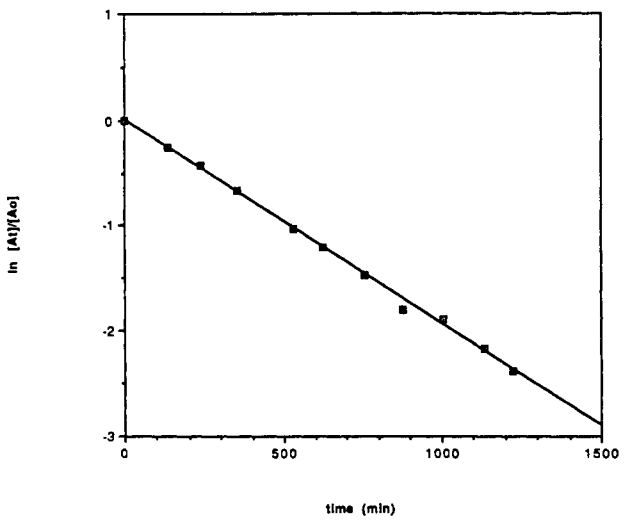

Figure 4. Plot of ln (A_t/A_0) versus time for the thermolysis of 1 at 160 °C in the presence of 3.5 equiv of di-*p*-tolylacetylene.

3) the oxygen and nitrogen atoms bound to zirconium are disordered about a pseudo mirror plane or C_2 axis passing through the zirconium and central nitrogen atom of the ring (see Experimental Section). Thus, the Zr–ON1 and Zr–ON2 distances are averages of Zr–O and Zr–N bond lengths. The C1–ON1 distance (1.285 (3) Å) is a reasonable average of that of C—O and C=N bonds. The metallacycle as a whole is nearly planar, with C2 and C9 (ipso carbons of the phenyl rings) bent only slightly (0.10 and 0.16 Å, respectively) out of the plane, in opposite directions. Attempts to generate the analogous metallacycle with trimethylacetonitrile in place of benzonitrile by this α-elimination method did not give an isolable compound (however, vide infra).

Mechanism of Thermal Decomposition of Cp^*_2Zr(Ph)(OH). To obtain insight into the mechanism of formation of the materials described above, we examined the rate of thermal decomposition of 1 and its deuterated analogue Cp^*_2Zr(Ph)(OD) (1-*d*) in the presence of the trapping agents just described. The reactions were monitored by ^1H NMR spectrometry in C_6D_6 at 160 °C in sealed NMR tubes using a standard one-pulse technique. The rate of loss of starting hydroxyphenyl compound 1 (1-*d*) was measured relative to an internal ferrocene or 1,3,5-trimethylbenzene standard. The observed rate constants for the separate thermolyses of 1 in the presence of 1,4-diphenyl-1,3-butadiyne, benzonitrile, and 3.3, 3.5, 7.5, and 11.0 equiv of di-*p*-tolylacetylene are given in Table IV. All reactions were monitored for greater than 3 half-lives; a representative plot is given in Figure 4. The results in Table IV and Figure 4 demonstrate that the disappearance of 1 is cleanly first order (average k_{obs} = (3.5 ± 0.2) × 10^{-5} s^{-1}) and is, within experimental error, independent of the type or concentration of trapping ligand. These results suggest a common intermediate for the formation of metallacycles **2a–4a** from 1. The rate of disappearance of 1 also appears to be independent of solvent polarity, as the corresponding rate constant in THF-d_8 is 3.57 × 10^{-5} s^{-1}. Similarly, this reaction is apparently not accelerated by added base, as the rate constant at 160 °C in C_6D_6 with 1 equiv of 4-*tert*-butylpyridine added is essentially unchanged (k_{obs} = 3.61 × 10^{-5} s^{-1}).

Scheme III

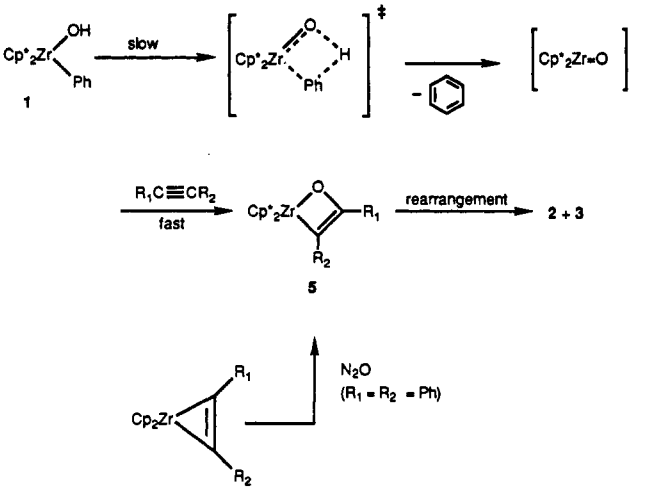

The volatile products formed in separate thermolyses of 1 and 1-*d* in toluene at 160 °C in the presence of excess diphenylacetylene indicate that C_6H_6 and C_6H_5D, respectively, are the exclusive (>97%) elimination products. This conclusion is based on a comparison of the GC–MS spectra (both fragmentation patterns and peak heights) of these products with authentic samples of C_6H_6 and C_6H_5D (the latter prepared from PhLi and D_2O). Further, studies of the rate of thermal decomposition of Cp^*_2Zr(Ph)(OD) at 160 °C in C_6D_6 (excess diphenylacetylene) reveal a substantially slower rate (average k_{obs} = (0.78 ± 0.2) × 10^{-5} s^{-1}; see Table IV) that is clearly first-order in 1-*d*. This rate reduction corresponds to the kinetic deuterium isotope effect k_H/k_D = 4.3 ± 0.1. The magnitude of this isotope effect indicates that an O–H (or O–D) bond undergoes cleavage in the transition state of the rate-determining step.

The above findings are most consistent with the mechanism shown in Scheme III. We envision the thermolysis of 1 proceeding by first-order, rate-determining elimination of benzene, leading to the transient species [$Cp^*_2Zr{=}O$]. By analogy to the behavior of [$Cp_2Zr{=}N(t\text{-}Bu)$],[4] we propose that alkynes react initially with the oxo intermediate to give oxametallacyclobutenes of type **5**. However, under the conditions necessary to generate [$Cp^*_2Zr{=}O$], these oxametallacycles are apparently unstable and rearrange to cyclometalated products **2a,b** and **3**.

This hypothesis requires that if **5a** could be independently synthesized, at 160 °C it should rearrange to **2a** at a kinetically competent rate. Fortunately, Hillhouse and co-workers reported recently that **5a** can be prepared by the reaction of zirconocene diphenylacetylene complex Cp^*_2Zr(PhCCPh) with N_2O[15] (we have also devised an alternative route to **5a**; vide infra). These workers kindly supplied us with a sample, and we found that its thermolysis (40 min at 160 °C) does result in a rather clean

(15) Vaughan, G. A.; Sofield, C. D.; Hillhouse, G. L.; Rheingold, A. L. *J. Am. Chem. Soc.* **1989**, *111*, 5491.

Scheme IV

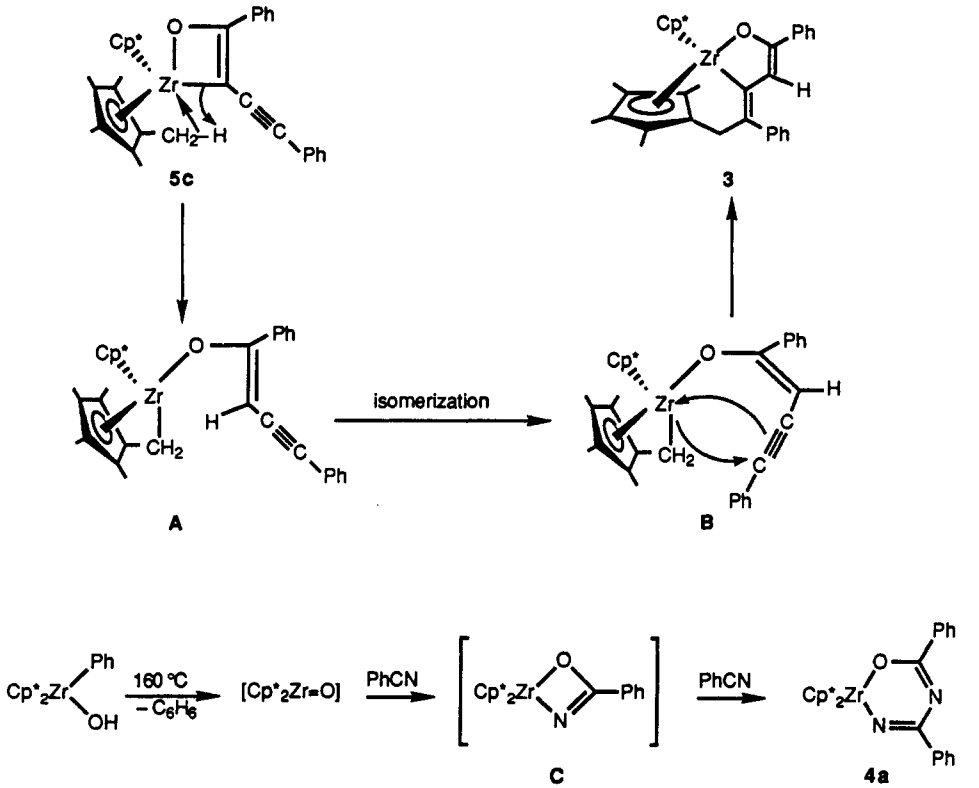

Scheme V

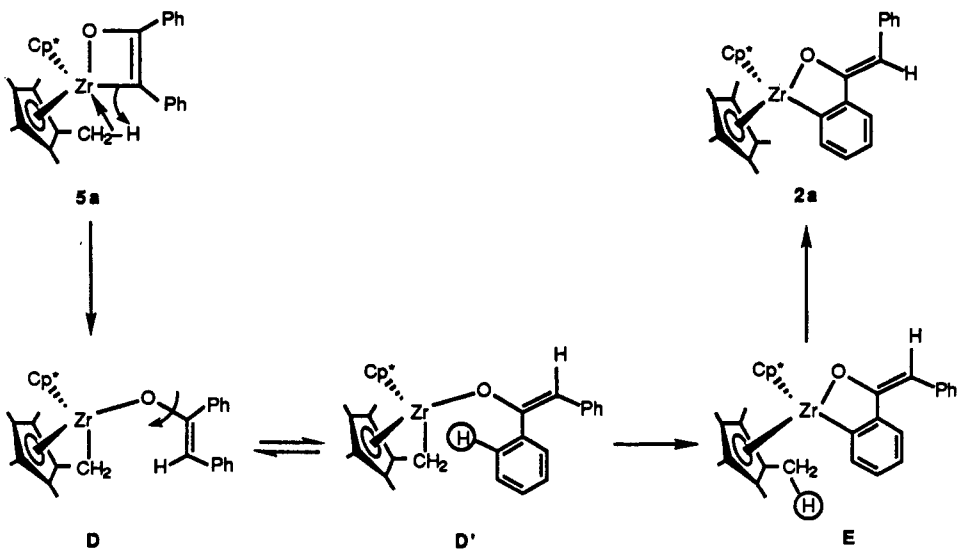

(85% by ^{1}H NMR spectrometry[16]) conversion to **2a**. The rapid (40 min) transformation of **5a** to **2a** at 160 °C is consistent with our inability to observe appreciable amounts of **5a** during the thermolysis of **1** (24 h to reach completion) and provides good evidence for the intermediacy of **5a** in the conversion of **1** to metallacycles **2**.

Thermal Rearrangement of Alkynyl-Substituted Metallacyclobutene 5c to Cp*-Ortho-Metalated Complex 3. The more perplexing mechanistic question concerns the pathway by which proposed intermediates **5** are converted to deep-seated rearrangement products **2** and **3**. We first consider the formation of **3**. One possible mechanism for this transformation, outlined in Scheme IV, involves the intimate involvement of the Cp* methyl C—H bonds. As mentioned above, we believe that metallacycle **5c** is formed initially by interaction of [Cp*$_2$Zr=O] with the alkyne. Addition of a Cp* methyl C—H bond across the Zr—C bond of **5c** would generate the Cp*-cyclometalated enolate A shown in Scheme IV. Cis–trans isomerizations about the enolate double bond followed by insertion of the remaining triple bond of the diyne into to the Zr–CH_2 bond of B leads to the observed product **3**. Benzonitrile insertion product **4a** presumably arises from initial cycloaddition of PhCN to the Zr=O bond to give the oxaazametallacyclobutene C; a second equivalent of PhCN would then insert into the Zr—N bond of C to give **4a**.

Thermal Rearrangement of Metallacyclobutenes 5a,b to Aryl-Ortho-Metalated Complexes 2a,b. A

(16) A small amount of PhCCPh is liberated during this thermolysis (consistent with the reduced yield of **2a**), suggesting that **5** may readily revert to the terminal oxo intermediate and free alkyne at these temperatures (vide infra).

Scheme VI

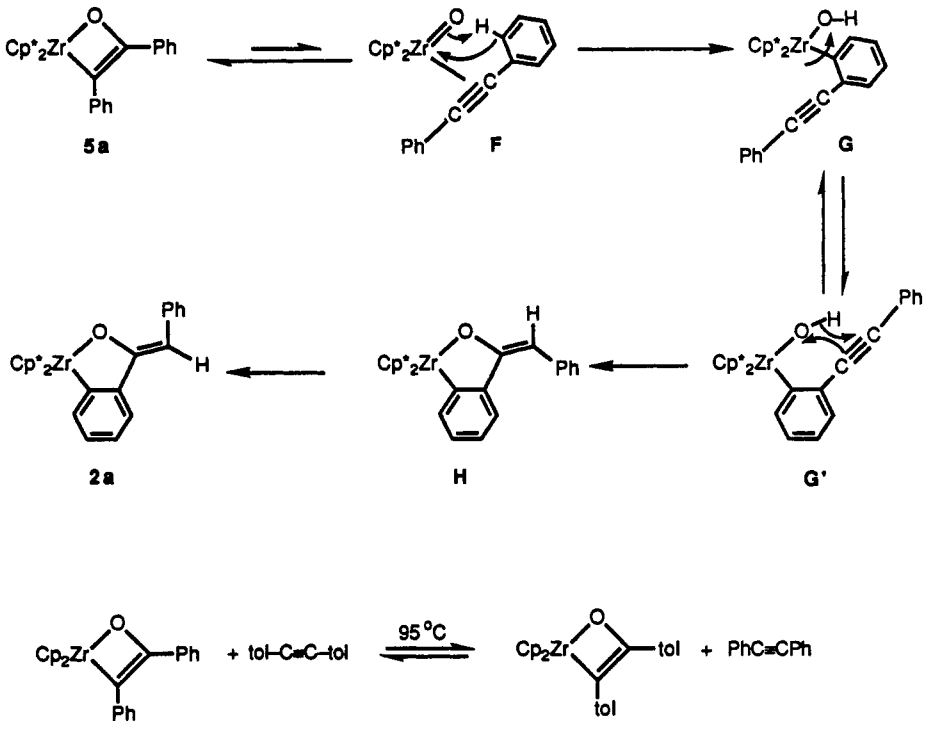

mechanism analogous to the one written for the conversion of alkynyl-substituted oxametallacycle **5c** to Cp*-cyclometalated complex **3** in Scheme IV can be postulated for the rearrangement of diphenyl-substituted oxametallacycle **5a** to **2a**; this is diagrammed in Scheme V. In this mechanism, complex **5a** is once again initially transformed to a Cp*-cyclometalated enolate (D) by formal addition of a C–H bond of a Cp* methyl group across the Zr–C bond of the metallacycle (i.e. transfer of an H atom to the vinylic position). Rotation about the oxygen–carbon bond in D would lead to a conformation (D′) in which the required phenyl ring lies in close proximity to the $Zr–CH_2$ bond of the cyclometalated species. Transfer of an ortho hydrogen from the phenyl ring to the $Zr–CH_2$ group by σ-bond metathesis generates E; subsequent isomerization about the enolate double bond then leads to the observed trans ortho-metalated metallacycles **2a,b**.

Similar mechanisms that utilize the hydrogen atoms of Cp* methyl groups to effect related transformations are well documented. For example, Bercaw et al.[17] have shown via kinetic and deuterium labeling studies that the thermal decomposition of $Cp^*_2Hf(CH_2Ph)_2$ proceeds ultimately through the cyclometalated benzyl complex $(\eta^5\text{-}C_5Me_5)(\eta^5{:}\eta^1\text{-}C_5Me_4CH_2)HfCH_2Ph$. This species then rearranges via a second σ-bond metathesis involving addition of an ortho C–H bond of the benzyl ligand across the weak cyclometalated Hf–C bond to form an ortho-metalated benzyl compound.[18]

We sought to test the mechanism proposed in Scheme V by performing the thermolysis of **1** in the presence of diphenylacetylene-d_{10}, with analysis of the products by ^1H and ^2H NMR spectrometry. Under the proposed mechanism one would expect no deuterium in the the vinylic position of **2a** (since its hydrogen would originate from the Cp* methyl groups) and 1 equiv of deuterium in the Cp* methyl groups due to the final ortho-metalation step. However, inspection of the ^1H NMR spectrum of the product **2a** isolated from the labeling study indicated only about 20% hydrogen at the vinylic position. Likewise, the ^2H NMR spectrum showed that only about 20% of one deuterium atom was incorporated into the Cp* methyl groups while the majority of the deuterium (80%) was located in the vinylic position. Thus, the mechanism outlined in Scheme V can account for at most only 20% of the reaction pathway. For the majority of the reaction, another mechanism must be operating.

One alternative that is consistent with the isotope tracer results is outlined in Scheme VI. It seems likely that the formation of **5** proceeds by initial coordination of alkyne to the unsaturated $[Cp^*_2Zr{=}O]$ complex to give oxo–alkyne adduct F as an intermediate in the formation of the oxametallacyclobutene. We suggest further that this adduct may be generated by the reverse process (fragmentation of the metallacyclobutene **5** at 160 °C). In support of this hypothesis, direct evidence has been obtained that the oxametallacyclobutene formation is indeed reversible. Heating (95 °C, C_6D_6) pure oxametallacyclobutene **5a** with a slight excess of di-*p*-tolylacetylene (1.4 equiv) in benzene yields after ca. 1.5 h a mixture of **5a** and the di-*p*-tolylacetylene metallacyclobutene **5b**, identified (but not isolated) primarily by the appearance of signals due to a new Cp* at 1.82 ppm and two new methyl groups at 2.23 and 2.12 ppm. At apparent equilibrium the metallacyclobutene product ratios are 53/47 (**5a**/**5b**) even in the presence of a slight excess (1.4 equiv) of di-*p*-tolylacetylene. In support of the conclusion that **5b** is formed in this reaction, at 95 °C the components of this mixture rearrange slowly (over about 20 h) to *both* ortho-metalated products **2a,b** (56/44 product ratio).

The **5a**/**5b** "alkyne-exchange" reaction indicates that the oxametallacyclobutenes **5** are in fact capable of reversion, most likely via the alkyne–oxo complex F illustrated in

(17) Bulls, A. R.; Schaefer, W. P.; Serfas, M.; Bercaw, J. E. *Organometallics* **1987**, *6*, 1219.

(18) For other apparent Cp*-mediated cleavages of group 4 metal–carbon bonds see ref 7b as well as: (a) Parkin, G.; Bercaw, J. E. *Organometallics* **1989**, *8*, 1172. (b) McDade, C.; Green, J. C.; Bercaw, J. E. *Organometallics* **1982**, *1*, 1629.

Scheme VI. As the second step en route to **2**, we propose selective ortho hydrogen C–H bond activation of one aryl ring; prior coordination of the alkyne to the terminal oxo complex would presumably place these ortho hydrogens nearest to the terminal oxo group. This C–H activation would yield zirconium hydroxy complex G. Rotation about the Zr–C(aryl) bond with subsequent cis addition of OH across the triple bond leads to cis ortho-metalated metallacycle H. Thermal cis–trans isomerization at 160 °C would then afford the observed trans product **2a**. In the case of the thermolysis of 1 in the presence of diphenylacetylene-d_{10}, this mechanism would account for the majority of deuterium being incorporated into the vinylic position.

Room-Temperature Generation and Trapping Reactions of [Cp*$_2$Zr=O]. The ready isomerization of metallacycles **5a,b** to ortho-metalated compounds at elevated temperatures during the thermolysis of 1, and our inability to isolate tractable products when alkyl-substituted alkynes or nitriles were employed in these thermolysis reactions, prompted us to find an alternative (preferably room-temperature) route to the oxo intermediate. As a first attempt, we decided to try the dehydrohalogenation of zirconocene hydroxy halides Cp*$_2$Zr(OH)(X) (**6**; X = Cl,[8] I).[19] It was hoped that deprotonation of **6** would generate the transient Cp*$_2$Zr(O$^-$)(X), which would then eliminate X$^-$ to yield the [Cp*$_2$Zr=O] intermediate. However, deprotonation of these species (X = Cl, I) with the hindered base KN(Si(CH$_3$)$_3$)$_2$ yielded only materials we believe to be the corresponding potassium salts [Cp*Zr(O$^-$)(X)][K$^+$] (sparingly soluble in benzene, soluble in THF). Although these organometallic anions were not fully characterized, they appear to be quite stable and do not undergo elimination of halide ion. For example, [Cp*Zr(O$^-$)(I)][K$^+$] and excess diphenylacetylene did not react at room temperature over several days.

In view of the difficulty of eliminating halide from the oxohalozirconium anions, we next decided to try to generate cationic salts [Cp*Zr(OH)$^+$] (or their solvates) by treatment of **6** (X = Cl) with silver trifluoromethanesulfonate (silver triflate; AgOSO$_2$CF$_3$). However, this reaction led to the zirconocene hydroxy triflate complex Cp*Zr(OH)(OSO$_2$CF$_3$) (**7**) in high yield. A new ^{1}H NMR (C$_6$D$_6$) Cp* resonance at 1.74 ppm and an OH resonance at 6.20 ppm distinguish this compound from the parent **6** (^{1}H NMR (C$_6$D$_6$): Cp*, 1.82 ppm; OH, 5.07 ppm). The presence of an OH stretch in the IR spectrum (3650 cm^{-1}) confirms the retention of the OH group during the metathesis reaction. Fortunately, due to the improved leaving ability of the triflate anion, deprotonation of **7** with KN(Si(CH$_3$)$_3$)$_2$ results in the successful generation of [Cp*$_2$Zr=O], as evidenced by its trapping with various alkynes and nitriles as shown in Scheme VII. For example, deprotonation of **7** in the presence of excess diphenylacetylene results in the clean formation (by ^{1}H NMR spectrometry) of **5a** (50% isolated yield); this compound is spectroscopically identical (^{1}H NMR) to that reported by Hillhouse.[15] Isolation of **5a** in the deprotonation of **7** provides further support for the intermediacy of oxametallacyclobutenes **5** in the reaction of 1 with diarylacetylenes at 160 °C. The new room-temperature route to [Cp$_2$*Zr=O] also allows us to use alkyl- as well as aryl-substituted acetylenes as traps for the oxo complex. Thus, deprotonation of **7** in the presence of 3–4 equiv of

Scheme VII

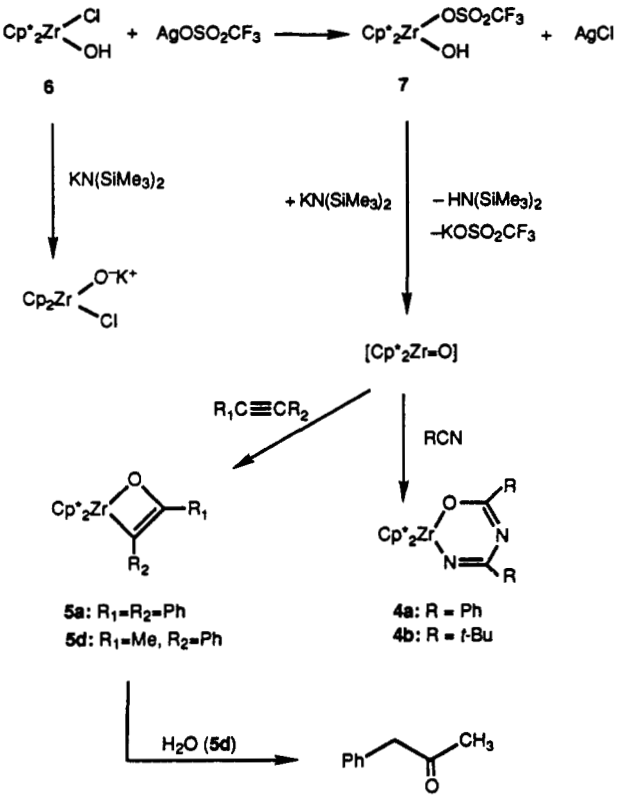

the unsymmetrical alkyne 1-phenyl-1-propyne afforded **5d** in 42% isolated yield.

Under these milder room-temperature conditions, the oxo/alkyne reaction is substantially cleaner. It leads to one regioisomer of **5d**, as only one Cp* (1.78 ppm), one Me group (2.33 ppm), and one set of phenyl resonances were observed by ^{1}H NMR analysis of the reaction mixture. The absolute regiochemistry of the trapped product was assigned by treating **5d** with 2 equiv of H$_2$O, which led to Cp*$_2$Zr(OH)$_2$[7a] and phenylacetone,[20] uncontaminated by PhCOCH$_2$CH$_3$. This anti-Markovnikov regiochemistry is analogous to that observed for the reaction of 1-phenyl-1-propyne with [Cp$_2$Zr=N(*t*-Bu)].[4] It appears to be a general trend that cycloaddition reactions of this type afford products that have the aryl substituent located in the position α to the metal.

The room-temperature deprotonation of **7** in the presence of excess benzonitrile afforded complex **4a**, spectroscopically identical to material isolated from the thermal reaction (160 °C) of 1 with benzonitrile described above. Further, deprotonation of **7** in the presence of 5 equiv of trimethylacetonitrile resulted in the clean formation of **4b**, an alkyl-substituted analogue of **4a**, in 80% yield. Proton and ^{13}C NMR spectra clearly show the presence of two inequivalent *tert*-butyl groups in this product, in accord with the structure shown in Scheme VII. The greater generality of this oxo generation method is evidenced here, as complex **4b** could not be isolated from the thermolysis reaction of 1, presumably because it does not survive the high-temperature reaction conditions.

Encouraged by the greater product accessibility obtained with this deprotonation procedure, we attempted to generate and isolate a stable Cp*$_2$(L)Zr=O species, analogous to the isoelectronic Cp$_2$(L)Zr=N(*t*-Bu) complexes that had been characterized earlier.[4] Deprotonation of **7** was carried

(19) Hillhouse has briefly mentioned a similar synthetic scheme directed toward the synthesis of terminal phosphinidene complexes (Vaughan, G. A.; Hillhouse, G. L.; Rheingold, A. L. *Organometallics* **1989**, *8*, 1760).

(20) This assignment was checked by comparison of the ^{1}H NMR spectrum with that of an authentic sample of phenylacetone.

Scheme VIII

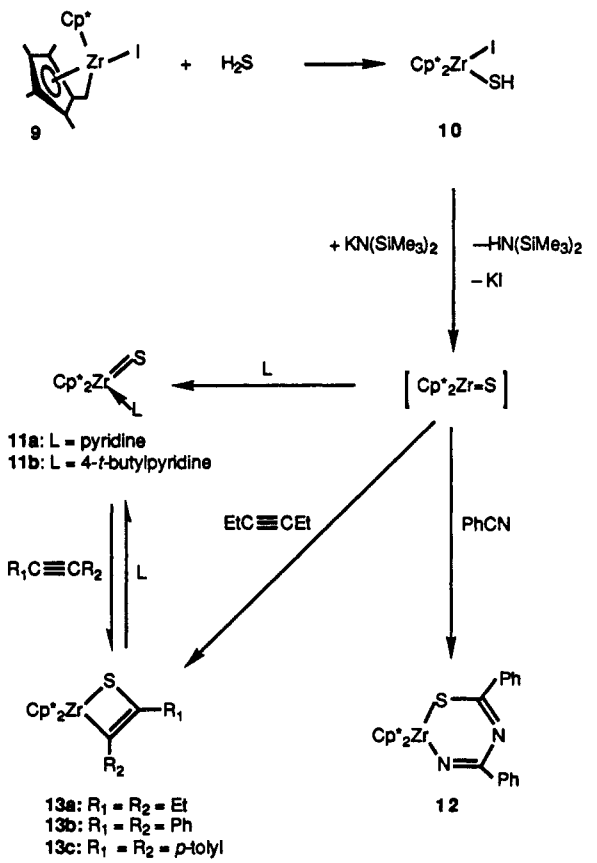

out in the presence of several dative ligands such as pyridine, 4-*tert*-butylpyridine, pyridine *N*-oxide, 4-(dimethylamino)pyridine (DMAP), and triphenylphosphine oxide, but none of these reactions resulted in the successful isolation of pure materials.[21] However, we have been able to generate and trap the isoelectronic $[Cp^*_2Zr{=}S]$ fragment in the presence of dative ligands, and we have examined its addition chemistry with alkynes and nitriles. This part of our study is discussed in the following section.

Room-Temperature Generation and Trapping Reactions of $[Cp^*_2Zr{=}S]$. The most convenient and direct route to $[Cp^*_2Zr{=}S]$ involves room-temperature dehydrohalogenation of $Cp^*_2Zr(SH)(I)$ (**10**). However, we have found that it is not a trivial matter to prepare unsymmetrical complexes of the type $Cp^*_2Zr(X)(Y)$ (X = halide, Y = other heteroatom), because substitution reactions of $Cp^*_2ZrX_2$ with small anionic nucleophiles (Y^-) generally produce mixtures of mono-, di-, and unsubstituted products. Thus, one must devise ways of introducing the heteroatom (Y) specifically. It appeared that treatment of cyclometalated compounds of the type $(\eta^5\text{-}C_5Me_5)(\eta^5{:}\eta^1\text{-}C_5Me_4CH_2)ZrX$ with the conjugate acid of these nucleophiles might protonate the cyclometalated Cp* and thus provide the most efficient route to unsymmetrical $Cp^*_2Zr(X)(Y)$ complexes. This is in fact the method used by Marks[7a] to prepare complex **1** in high yield.

The synthesis of our target precursor $(\eta^5\text{-}C_5Me_5)(\eta^5{:}\eta^1\text{-}C_5Me_4CH_2)ZrI$ is based primarily on a similar synthetic scheme used by Bercaw et al. to generate the cyclometalated hafnium iodides $(\eta^5\text{-}C_5Me_5)(\eta^5{:}\eta^1\text{-}C_5Me_4CH_2)HfI$.[17] We began by treating $Cp^*_2ZrI_2$[7a] with

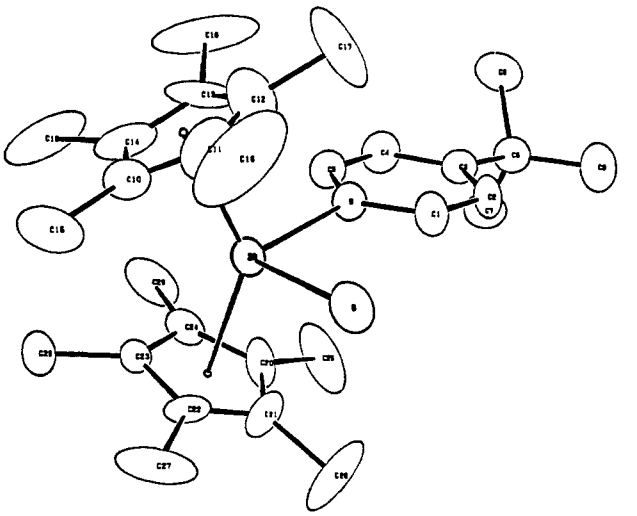

Figure 5. ORTEP diagram of terminal sulfido 4-*tert*-butylpyridine adduct complex **11b** with 30% probability thermal ellipsoids. The diagram shows the numbering scheme used in the tables.

1.1 equiv of neopentyllithium[22] in benzene to give $Cp^*_2Zr(neopentyl)(I)$ (**8**) in 90% isolated yield. Thermolysis of **8** at 140 °C in benzene for 4 h led to the liberation of neopentane and the generation of the intensely purple cyclometalated iodide $(\eta^5\text{-}C_5Me_5)(\eta^5{:}\eta^1\text{-}C_5Me_4CH_2)ZrI$ (**9**; Scheme VIII) in 81% yield. The presence of two upfield doublets in the proton NMR spectrum (2.21 and 1.56 ppm) due to the diastereotopic methylene hydrogens (as well as the general pattern typical of cyclometalated structures) and a resonance at 70.4 ppm in the ^{13}C NMR spectrum (typical for CH_2 bound to Zr) confirmed the cyclometalated nature of **9**. Subsequent treatment of **9** with a slight excess of H_2S gave the iodo hydrosulfido complex **10** in 85% isolated yield as a yellow crystalline solid. Singlet ^1H NMR resonances due to Cp* (1.89 ppm) and SH (2.69 ppm) protons are the only peaks present. Unfortunately, the IR stretch due to the SH group (these appear near 2600 cm^{-1} but are often quite weak[23]) could not be unambiguously assigned.

In contrast to the behavior of the analogous chloro hydroxide **6**, deprotonation of **10** with $K(N(SiMe_3)_2)$ serves as a useful source of $[Cp^*_2Zr{=}S]$. Most importantly, dehydrohalogenation of **10** in the presence of excess pyridine or 4-*tert*-butylpyridine afforded monomeric terminal sulfido complexes **11a** and **11b**, respectively, in good yield. The ^1H NMR spectra of these complexes are characterized by a single resonance due to the equivalent Cp* groups but possess a pattern in the aromatic region indicating that all pyridine hydrogens are inequivalent. This suggests that the pyridine ligand is firmly bound and is rotating slowly on to the NMR time scale at 25 °C.

An X-ray crystal structure determination was carried out on **11b** to confirm the proposed unique Zr=S bonding mode. Orange single crystals were obtained by layering hexane on top of a saturated benzene solution of **11b**. Crystal and X-ray data collection parameters are provided in Table I; selected interatomic distances and angles can be found in Tables II and III, respectively. Inspection of the ORTEP diagram shown in Figure 5 shows that the pyridine ligand is trapped in the cleft formed by the Cp* groups. The NMR inequivalence of the pyridine hydrogens suggests that this structure is maintained in solution. The Zr—S distance of 2.316 (1) Å in **11b** is at least 0.1 Å

(21) Monitoring by ^1H NMR spectrometry provides evidence that a triphenylphosphine oxide adduct, $Cp^*_2(OPPh_3)Zr{=}O$, can be generated by deprotonation of **2** in the presence of excess phosphine oxide, but attempts to isolate pure material were unsuccessful.

(22) Schrock, R. R.; Fellmann, J. D. *J. Am. Chem. Soc.* **1978**, *100*, 3359.
(23) Silverstein, R. M.; Bassler, G. C.; Morrill, T. C. *Spectrometric Identification of Organic Compounds*, Wiley: New York, 1981; p 131.

shorter than observed Zr—S single-bond distances (typically bond lengths range from 2.42 to 2.50 Å[24]), thus confirming the multiply bonded nature of the Zr—S fragment. To our knowledge, this is the first group 4 monomeric terminal sulfido complex to be structurally characterized. In addition, it is a rare example of a terminal sulfido compound that exhibits reactivity toward organic molecules (see below). The Zr–N distance (2.341 (4) Å) is similar to that of other Zr(IV) pyridine adducts,[25] and the N–Zr–S angle is 91.85 (9)°. The plane containing the Zr, S, and N atoms lies in the cleft of the Cp* ligands and is approximately equidistant from each Cp*. However, the plane of the pyridine ligand itself is tilted by ca. 10° with respect to this plane so that the pyridine ligand is canted toward one Cp* ligand.

Having confirmed the intermediacy of [Cp^*_2Zr=S] in the dehydrohalogenation of **10** by trapping it with dative ligands, we then attempted to trap this intermediate with other organic molecules, in analogy to the oxo work described above. We first attempted to trap [Cp^*_2Zr=S] with benzonitrile. Dehydrohalogenation of **10** in the presence of excess benzonitrile afforded the thiaazametallacycle **12** as a yellow-orange solid in 79% yield after recrystallization (Scheme VIII). This compound possesses a ^{1}H NMR spectrum that is virtually identical to that found for **4a**, supporting our formulation of the latter complex as the six-membered oxametallacycle shown in Scheme VII. A similar dehydrohalogenation reaction of **10** in the presence of excess trimethylacetonitrile did not yield a clean product.

Parallels in the chemistry of the oxo and sulfido complexes include the generation of metallacyclobutene compounds. Thus, generation of the terminal sulfido intermediate by dehydrohalogenation of **10** in the presence of 3-hexyne forms the thiametallacyclobutene **13a** (Scheme VIII), an orange crystalline solid isolated in 35% yield after recrystallization from ether. Its ^{1}H NMR (C_6D_6) spectrum is characterized by a single Cp* resonance at 1.79 ppm, as well as two triplets at 1.11 and 1.42 ppm, respectively, and two overlapping quartets (2.62–2.51 ppm) due to the inequivalent ethyl groups. This spectrum is consistent with the formulation of **13a** as diagrammed in Scheme VIII, but a zirconocene terminal sulfido–alkyne adduct in which the alkyne is unsymmetrically bound cannot be strictly ruled out (vide infra) on the basis of NMR evidence.

Unexpectedly, similar reactions in which [Cp^*_2Zr=S] is generated by dehydrohalogenation of **10** at room temperature in the presence of excess diarylacetylenes such as diphenylacetylene do not afford metallacycles of type **13** but instead yield complex mixtures of products. We have found, however, that heating terminal sulfido complexes **11** at 85 °C for ca. 12 h in the presence of diphenyl- or di-*p*-tolylacetylene affords thiametallacyclobutenes **13b,c** in good yield. Surprisingly, even in the presence of an excess (3–4 equiv) of diarylacetylenes, a small amount (ca. 5%) of **11** remains even after prolonged heating. Consistent with this observation, heating terminal sulfide **11a** in the presence of 3 equiv of 3-hexyne yielded a 62:38 ratio (by ^{1}H NMR spectrometry) of **13a**:**11a** even after

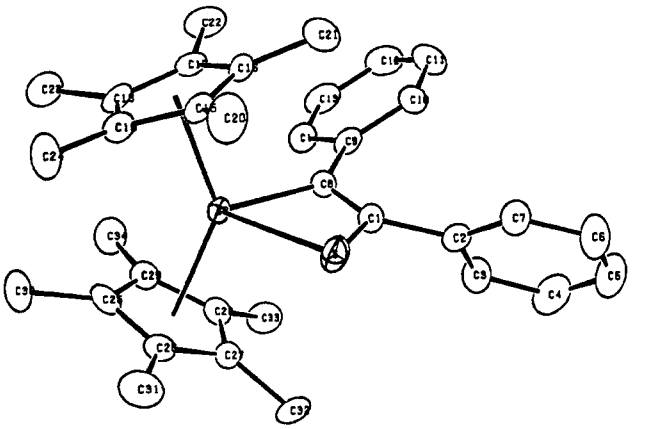

Figure 6. ORTEP diagram of diphenylacetylene insertion product **13b** with 50% probability thermal ellipsoids. The diagram shows the numbering scheme used in the tables.

lengthy heating at 45 °C. This ratio did not change after heating at 85 °C for several hours. Thus, it appears that the monomeric terminal sufido complex (**11**)–metallacyclobutene (**13**) transformation is reversible, as it is in the corresponding nitrogen and oxygen complexes. In contrast to the first-row systems, however, the terminal sulfido complex–alkyne mixtures and thiametallacycles have comparable free energies.[26,27]

This reversibility was confirmed by the observation that **13a** can be cleanly and nearly completely (95% by ^{1}H NMR spectrometry) converted into **11b** by simply warming (45 °C) the thiametallacycle in the presence of 3 equiv of 4-*tert*-butylpyridine (C_6D_6, 2 h). Additionally, heating diphenylacetylene adduct **13b** with ca. 7 equiv of 4-*tert*-butylpyridine at 85 °C for 12 h resulted in the generation of a 65:35 ratio of **13b**:**11b**. Thus, it appears that the diphenylmetallacyclobutene **13b** is inherently more stable than the corresponding 3-hexyne complex **13a**, yet there is a barrier to the formation of **13b** inasmuch as the room-temperature dehydrohalogenation of **10** in the presence of diphenylacetylene does not yield **13b**. The reason for this rather pronounced difference between the alkyl- and aryl-substituted acetylene addition products **13** is unclear at present. Nevertheless, *these experiments demonstrate the stability of the Zr=S linkage and suggest that it is more stable than the Zr=O group with respect to cycloaddition reactions with alkynes.* This is quite unexpected, given the commonly accepted notion about the oxophilicity of these early transition metals and the (presumed) comparatively poor ability of sulfur to π-bond to these early metals.

Because of the reversibility noted above, and because recent work from Mayer's group on oxorhenium systems has demonstrated that terminal oxo and alkyne functionalities can coexist on the same metal center without undergoing cycloaddition or other types of addition chemistry,[28] we felt it necessary to carry out an X-ray crystal

(24) For representative Zr–S distances see: (a) Kovacs, J. A.; Bergman, R. G. *J. Am. Chem. Soc.* **1989**, *111*, 1131. (b) Hey, E.; Lappert, M. F.; Atwood, J. L.; Bott, S. G. *J. Chem. Soc., Chem. Commun.* **1987**, 421. (c) Bottomley, F.; Drummond, D. F.; Egharevba, G. O.; White, P. S. *Organometallics* **1986**, *5*, 1620. (d) Coucouvanis, D.; Lester, R. K.; Kanatzidis, M. G.; Kessissoglou, D. P. *J. Am. Chem. Soc.* **1985**, *107*, 8279. (e) Coucouvanis, D.; Hadjikyriacou, A.; Kanatzidis, M. G. *J. Chem. Soc., Chem. Commun.* **1985**, 1224.

(25) The Zr–N distance in $Cp_2Zr(NC_5H_5)(PhNNPh)$ is, for example, 2.431 Å (Walsh, P. J.; Hollander, F. J.; Bergman, R. G. *J. Am. Chem. Soc.* **1990**, *112*, 894).

(26) The oxa- and azametallacyclobutenes do undergo alkyne exchange, indicating that the monomeric oxo and imido intermediates can be generated from the metallacyclobutenes. However, in these latter cases dative ligands do not effectively compete with the alkyne for the unsaturated intermediates and the equilibria lie almost totally on the side of the respective metallacyclobutenes.

(27) Attempts to generate Cp^*_2Zr=S in the absence of trapping agents led to very complex mixtures of products. We were not able to determine reliably, by comparison of NMR spectra with published data, whether this mixture contained any substantial amount of the known dinuclear complex $[Cp^*_2Zr(\mu\text{-S})]_2$; cf. ref 24c and: Beckhaus, R.; Thiele, K.-H. *Z. Anorg. Allg. Chem.* **1989**, *573*, 195.

(28) Several rhenium–oxo–alkyne complexes are known (see: Mayer, J. M.; Thorn, D. L.; Tulip, T. H. *J. Am. Chem. Soc.* **1985**, *107*, 7454).

structure determination of **13** to confirm its proposed metallacyclic nature and to rule out the possibility that these complexes exist as zirconium–sulfido–alkyne adducts. Large blocklike red crystals of **13b** were obtained after layering hexane on top of a saturated solution of the compound, and these were found to be satisfactory for an X-ray diffraction study. Crystal and X-ray data collection parameters are provided in Table I, while selected interatomic distances and angles can be found in Tables II and III, respectively. An ORTEP diagram is provided in Figure 6 and clearly demonstrates the metallacyclic nature of this complex. The C–S bond length (1.829 (5) Å) is typical for a C–S single bond. The Zr–S distance has lengthened considerably from that observed in **11b** (from 2.316 (1) to 2.505 (1) Å) and is entirely consistent with the change in Zr–S bond order form 2 to 1.[24] The Zr–C8 bond length (2.226 (4) Å) is quite normal for the metallacycles of this type, while the C1–C8 distance (1.330 (6) Å) is in the range expected for a C=C bond. The Zr–S–C1–C8 metallacycle is nearly planar with S and C8 "raised" (0.03 and 0.05 Å) and Zr and C1 (0.02 and 0.06 Å) "lowered" only slightly out of the plane.

We have carried out some preliminary experiments designed to explore the possibility of generating $[Cp^*_2Zr{=}S]$ by the α-elimination of benzene from $Cp^*_2Zr(Ph)(SH)$ (**14**). It appears that **14** can be generated in a fashion similar to that reported for zirconocene hydroxy phenyl complex **1**,[7a] by treatment of $(\eta^5\text{-}C_5Me_5)(\eta^5{:}\eta^1\text{-}C_5Me_4CH_2)Zr(Ph)$[7b] with 1.0 equiv of H_2S (via a known volume bulb). The ^1H NMR spectrum of the product formed in this reaction exhibits phenyl region, Cp* (1.72 ppm), and SH (2.65 ppm) signals consistent with its formulation as hydrosulfido complex **14**. However, this compound was not isolated, as it is thermally unstable and decomposes at room temperature in benzene to a mixture of $Cp^*_2Zr(SH)_2$, a new compound formulated as the bridging sulfido dimer $(Cp^*_2(SH)Zr)_2(\mu\text{-}S)$ (**15**), and other unidentified materials. Complex **15** can be obtained directly and cleanly by heating $Cp^*_2ZrPh_2$ with 1.5 equiv of H_2S for 4 h at 85 °C. It is characterized by an ^1H NMR spectrum (C_6D_6) that shows inequivalent Cp* groups (1.98 and 1.94 ppm) and a single SH resonance at 1.35 ppm (integrated to 2 H per molecule). The stoichiometry of the above reaction (1.5 equiv of H_2S/1.0 equiv of Zr) is also in accord with the formulation of **15** as the bridging sulfido dimer. The inequivalence of the Cp* groups is similar to that observed in some closely related bridging oxo compounds such as $(Cp^*_2(H)Zr)_2(\mu\text{-}O)$.[29]

Generation and subsequent decomposition of **14** in the presence of 3-hexyne, 1-phenyl-1-propyne, or diphenylacetylene did not yield metallacycles such as **13**, suggesting that $[Cp^*_2Zr{=}S]$ is not involved in the formation of dimer **15** and that (unlike $Cp_2Zr(OH)Ph$) α-elimination is not a dominant pathway in its thermolysis. A more likely scenario for the conversion of **14** to **15** involves simple protonation of a bound phenyl group of **14** by a bound and probably quite acidic SH functionality on a neighboring Zr center, resulting in the formation of the $Zr(\mu\text{-}S)Zr$ bridge of **15** directly.

Summary and Conclusions

This paper outlines synthetic procedures that result in the successful generation of the oxo complex $[Cp^*_2Zr{=}O]$ and its sulfur analogue $[Cp^*_2Zr{=}S]$. We have found these unsaturated intermediates to be unusually reactive toward organic compounds. The generation of $[Cp^*_2Zr{=}O]$ has been accomplished in two ways. First, the α-elimination of benzene from $Cp^*_2Zr(Ph)(OH)$ (**1**) at 160 °C in the presence of diphenylacetylene or di-*p*-tolylacetylene leads to ortho-metalated oxametallacycles **2a,b**. Evidence has been presented that the initially formed species in this reaction is $[Cp^*_2Zr{=}O]$, and this species reacts with diarylacetylenes to give oxametallacyclobutenes of type **5**. However, these rearrange to ortho-metalated structures **2** at the elevated temperatures necessary for the α-elimination of benzene from **1**. Generation of $[Cp^*_2Zr{=}O]$ at 160 °C in the presence of 1,4-diphenyl-1,3-butadiyne yields the complex metallacycle **3**, in which one Cp* ligand has been incorporated into the coordinated enolate moiety. A similar thermolysis reaction, this time carried out in the presence of excess benzonitrile, yields the six-membered oxaazametallacycle **4a** formed from insertion of 2 equiv of PhCN into the Zr=O fragment. The connectivities of complexes **2a**, **3**, and **4a** were confirmed by X-ray structure determinations.

Second, room-temperature deprotonation of $Cp^*_2Zr(OH)(OSO_2CF_3)$ with $KN(SiMe_3)$ also results in the generation of $[Cp^*_2Zr{=}O]$. This milder, low-temperature route is useful for the synthesis of the metallacyclobutenes **5a,b**; in addition, the insertion of the unsymmetrical alkyne 1-phenyl-1-propyne into the Zr=O bond proceeds regiospecifically, yielding only phenylacetone upon hydrolysis. The reaction of $[Cp^*_2Zr{=}O]$ with benzonitrile and trimethylacetonitrile yields metallacycles **4a,b** in good yield. The greater product accessibility of this room-temperature method compared to that of the thermolysis reaction is exemplified here (and above in the generation of **5**), as **4b** cannot be isolated from the 160 °C α-elimination reaction. We have been unable to isolate stable terminal oxo complexes $Cp^*_2(L)Zr{=}O$ (L = dative ligands) in pure form, but the observed low-temperature reactivity of the $[Cp^*_2Zr{=}O]$ intermediate with alkynes and nitriles underscores the inherent reactivity of this Zr=O linkage. Kinetic, alkyne-exchange, and isotope-labeling studies support a mechanism involving direct elimination of benzene from **1** in the thermal generation of $[Cp^*_2Zr{=}O]$. They also suggest that the rearrangement of the oxametallacyclobutenes **5a,b** proceeds by initial reversion of the metallacycle to an oxo–alkyne complex followed by attack of oxygen on the phenyl ring of the alkyne.

We have also shown that $[Cp^*_2Zr{=}S]$, an isoelectronic analogue of the $[Cp^*_2Zr{=}O]$ complex, can be generated. Like the analogous imido complexes $[Cp_2Zr{=}N\text{-}t\text{-}Bu]$ studied earlier,[4] the sulfido complexes form dative-ligand adducts $Cp^*_2(L)Zr{=}S$ (L = pyridine (**11a**), 4-*tert*-butylpyridine (**11b**)) that can be isolated and fully characterized. An X-ray structure determination of **11b** confirmed the unusual Zr=S bonding mode and represents a rare example of this structural type among group 4 metals. Like its oxo analogue, the Zr=S multiply bonded linkage displays unprecedented reactivity toward organic molecules (including nitriles and alkynes), as evidenced by the formation of the thiaazametallacycle **12** and the thiametallacyclobutenes **13a–c**. The latter structural type was confirmed by an X-ray structure determination of **13b**. Metallacycles in all three series—nitrogen, oxygen, and sulfur—undergo thermal reversion to the $[Cp^*_2Zr{=}X]$ intermediate and alkyne. In the case of the imido and oxo species, this was evidenced by interconversion of one metallacycle with another upon treatment with a different alkyne. However, the relative propensity for cycloreversion is most unexpected. Cycloreversion of the zirconium oxo and imido complexes requires heating to temperatures near 90 °C. In contrast, the thiametallacyclobutenes undergo reversion

(29) Hillhouse, G. L.; Bercaw, J. E. *J. Am. Chem. Soc.* **1984**, *106*, 5472.

under much milder conditions and in fact can be readily converted into monomeric terminal sulfido complexes 11 and free alkyne by reaction of the metallacyclobutene with pyridines at room temperature. This suggests that of the three types of complexes so far investigated in the $Cp^*_2Zr{=}X$ series (X = NR, O, S), the sulfido species are the most stable.

The terminal oxo and sulfido intermediates generated here possess unprecedented reactivity toward organic molecules, and their generation bodes well for the synthesis of similarly reactive metal–heteroatom multiple bonds. Also, like their nitrogen-containing counterparts, these oxa- and thiametallacyclobutenes promise to exhibit rich insertion chemistry of unsaturated organic fragments into the Zr–C or Zr–O(S) bonds.

Experimental Section

General Considerations. Unless otherwise noted, all manipulations were carried out under an inert atmosphere in a Vacuum Atmospheres 553-2 drybox with attached M6-40-1H Dri-Train or by using standard Schlenk or vacuum-line techniques. ^1H NMR spectra were obtained on the 300-, 400-, and 500-MHz Fourier transform spectrometers at the University of California, Berkeley (UCB), NMR facility. The 300-MHz instrument was constructed by Mr. Rudi Nunlist and interfaced with a Nicolet 1180 computer. The 400- and 500-MHz instruments were commercial Bruker AM series spectrometers. Complete ^1H and ^{13}C NMR data for all new compounds are contained in Tables V and VI, respectively.

Solution infrared spectra were obtained in 0.1-mm NaCl sealed cells on a Perkin-Elmer Model 510 FT-IR spectrometer. Mass spectroscopic (MS) analyses were obtained at the UCB mass spectrometry facility on AEI MS-12 and Kratos MS-50 mass spectrometers. Elemental analyses were obtained from the UCB Microanalytical Laboratory, but in several cases we encountered difficulty (as have other investigators) in obtaining satisfactory elemental analyses on zirconium complexes, due presumably to incomplete combustion. Sealed NMR tubes were prepared by flame-sealing Wilmad 505-PP and 504-PP tubes which were attached via Cajon adapters directly to Kontes vacuum stopcocks.[30] Known volume bulb vacuum transfers were accomplished with an MKS Baratron attached to a high-vacuum line.

Unless otherwise specified, all reagents were purchased from commercial suppliers and used without further purification. Ferrocene (Aldrich) and diphenylacetylene-d_{10} (Merck) were sublimed prior to use. Pentane and hexanes (UV grade, alkene free) were distilled from $LiAlH_4$ under nitrogen. Benzene, toluene, ether, and tetrahydrofuran were distilled from sodium–benzophenone ketyl under nitrogen. Deuterated solvents for use in NMR experiments were dried, as were their protiated analogues, but were vacuum-transferred from the drying agent. The compounds $Cp^*_2ZrCl_2$,[7a] $Cp^*_2ZrI_2$,[7a] $Cp^*_2Zr(Ph)(OH)$,[7a] $Cp^*_2Zr(OH)(Cl)$,[8] and neopentyllithium[22] were prepared by published methods.

Kinetic Experiments. All reactions were followed by monitoring the decrease in integrated ^1H NMR intensity of the pentamethylcyclopentadienyl resonance of the starting complex $Cp^*_2Zr(Ph)(OH)$ (1) or $Cp^*_2Zr(Ph)(OD)$ (1-*d*) with respect to internal $(\eta^5\text{-}C_5H_5)_2Fe$ or 1,3,5-trimethylbenzene standard. ^1H NMR spectra were recorded at timed intervals by using the Nicolet 300-MHz instrument described above employing a one-pulse experiment. The reaction temperature was maintained by using a constant-temperature oil bath controlled by a thermoregulator and was observed to be constant to ±0.2 °C. A typical experiment involved 10 mg of zirconium complex 1 (or 1-*d*) and 5 mg of ferrocene or an equivalent amount of 1,3,5-trimethylbenzene dissolved in 0.5 mL of benzene-d_6. The required equivalent of various trapping agents were added (see Table IV), and the NMR tubes were sealed under vacuum. Total submersion in the oil bath insured a uniform temperature over the length of the NMR tubes. Spectra were recorded at various timed intervals, and spectra at each point in time were recorded at least twice and the average intensity was used to calculate the values of k_{obs} given in Table IV.

Synthesis of $Cp^*_2Zr(Ph)(OD)$ (1-*d*). This compound was prepared analogously in a yield comparable to that reported for $Cp^*_2Zr(Ph)(OH)$ (1)[7a] with D_2O (freshly opened bottle) used in place of H_2O. Integration of the residual OH resonance versus Cp* and phenyl resonances indicated that the product was >97% $Cp^*_2Zr(Ph)(OD)$.

Synthesis of $Cp^*_2Zr(OC(o\text{-}C_6H_4){=}C(Ph)(H))$ (2a). $Cp^*_2Zr(Ph)(OH)$ (1; 300 mg, 0.658 mmol) and diphenylacetylene (350 mg, 1.96 mmol) were dissolved in 25 mL of benzene; the mixture was placed in a Pyrex bomb and freeze–pump degassed. This solution was heated at 160 °C for 2 days, and the solvent was removed by lyophilization. The residue was dissolved in 20 mL of ether and the solution filtered and concentrated in vacuo to a volume of 10 mL. Cooling to −40 °C overnight resulted in the deposition of orange-yellow crystals. These were washed with cold hexane (2 mL), and the solvent was removed in vacuo, yielding 250 mg (68%) of pure compound: IR (C_6H_6) 2907, 1564, 1444, 1380, 1370, 1264, 1253, 1201, 1112, 1085, 1026 cm^{-1}; MS (EI) m/e 554 (M^+), 105 (base). Anal. Calcd for $C_{34}H_{40}OZr$: C, 73.46; H, 7.25. Found: C, 73.32; H, 7.25.

X-ray Structural Data for 2a. Large yellow-orange crystals of **2a** were obtained by slow crystallization from ether. Fragments cleaved from some of these crystals were mounted in thin-walled glass capillaries in an inert-atmosphere glovebox and then flame-sealed. Preliminary precession photographs indicated monoclinic Laue symmetry and yielded approximate cell dimensions. The crystal used for data collection was then transferred to our Enraf-Nonius CAD-4 diffractometer and centered in the beam.[31] Automatic peak search and indexing procedures yielded the monoclinic reduced primitive cell. The final cell parameters and specific data collection parameters for this data set are given in Table I.[11]

The 4205 raw intensity data were converted to structure factor amplitudes and their esd's by correction for scan speed, background, and Lorentz-polarization effects. No correction for crystal decomposition was necessary. Inspection of the azimuthal scan data showed a variation $I_{min}/I_{max} = \pm 2\%$ for the average curve. No absorption correction was applied. Inspection of the systematic absences indicated uniquely space group $P2_1/n$. Removal of systematically absent and redundant data left 3797 unique data in the final data set. The structure was solved by Patterson methods and refined via standard least-squares and Fourier techniques. In a difference Fourier map calculated following the refinement of all non-hydrogen atoms with anisotropic thermal parameters, peaks were found corresponding to most of the hydrogen atoms. Hydrogen atoms were assigned idealized locations and values of B_{iso} approximately 1.3 times the B_{eqv} values of the atoms to which they were attached; they were included in the structure factor calculations but not refined.

The final residuals for 325 variables refined against 3169 data for which $F^2 > 3\sigma(F^2)$ wre $R = 2.72\%$, $R_w = 3.98\%$, and GOF = 2.05. The R value for all 3797 data was 4.81%. In the final cycles of refinement the two most intense reflections were removed from the refinement due to perceived effects of secondary extinction. The quantity minimized by the least-squares program was $\sum w(|F_o| - |F_c|)^2$, where w is the weight of a given observation. The p factor, used to reduce the weight of intense reflections, was set to 0.03 throughout the refinement. The analytical forms of the scattering factor tables for the neutral atoms were used, and all scattering factors were corrected for both the real and imaginary component of anomalous dispersion.[30b]

Inspection of the residuals ordered in angles of $(\sin\theta)/\lambda$, $|F_o|$, and parity and value of the individual indexes showed no unusual

(30) Bergman, R. G.; Buchanan, J. M.; McGhee, W. D.; Periana, R. A.; Seidler, P. F.; Trost, M. K.; Wenzel, T. T. In *Experimental Organometallic Chemistry: A Practicum in Synthesis and Characterization*; Wayda, A. L., Darensbourg, M. Y., Eds.; ACS Symposium Series 357; American Chemical Society: Washington, DC, 1987; p 227.

(31) For a description of the X-ray diffraction and analysis protocols used, see: (a) Hersh, W. H.; Hollander, F. J.; Bergman, R. G. *J. Am. Chem. Soc.* **1983**, *105*, 5834. (b) Cromer, D. T.; Waber, J. T. *International Tables for X-ray Crystallography*; Kynoch Press: Birmingham, England, 1974; Vol. IV, Table 2.2B.

Table V. ^1H NMR Spectroscopic Data (25 °C)[a]

assignt	mult (*J*, Hz)	δ ppm; rel int	assignt	mult (*J*, Hz)	δ ppm; rel int
		$Cp^*_2Zr(OC(o\text{-}C_6H_4){=}C(Ph)(H))$ (**2a**)			
$\eta^5\text{-}C_5(CH_3)_5$	s	1.67; 30 H	aryl	t (7.91)	7.39; 2 H
$C{=}C(Ph)(H)$	s	6.27; 1 H		m	7.65; 1 H
aryl	m	6.83; 1 H		d (8.18)	7.90; 2 H
	m	7.09–7.15; 3 H			
		$Cp^*_2Zr(OC(o\text{-}C_6H_4CH_3){=}C(Tol)(H))$ (**2b**)			
$\eta^5\text{-}C_5(CH_3)_5$	s	1.72; 30 H	aryl	s	6.70; 1 H
p-tolyl CH_3	s	2.28; 3 H		dd (8.07, 1.31)	6.93; 1 H
	s	2.34; 3 H		d (8.10)	7.18; 2 H
$C{=}C(Tol)(H)$	s	6.24; 1 H		d (8.09)	7.60; 1 H
				d (8.17)	7.82; 2 H
		$(\eta^5\text{-}C_5(CH_3)_5)Zr(OC(Ph){=}C(H)C(Ph)(\eta^5\text{-}C_5(CH_3)_4CH_2))$ (**3**)			
$\eta^5\text{-}C_5(CH_3)_5$	s	1.92; 15 H	$C{=}C(Tol)(H)$	s	6.87; 1 H
$\eta^5\text{-}C_5(CH_3)_4CH_2$	s	1.66; 3 H	*p* phenyl	t (7.27)	7.05; 1 H
	s	1.97; 3 H		t (7.36)	7.09; 1 H
	s	2.16; 3 H	*m* phenyl	t (7.61)	7.14; 2 H
	s	2.23; 3 H		t (7.73)	7.26; 2 H
$(\eta^5\text{-}C_5(CH_3)_4CH_2)$	d (17.81)	3.50; 1 H	*o* phenyl	d (7.15)	7.45; 2 H
	d (17.82)	3.81; 1 H		d (7.30)	7.51; 2 H
		$Cp^*_2Zr(OC(Ph){=}NC(Ph){=}N)$ (**4a**)			
$\eta^5\text{-}C_5(CH_3)_5$	s	1.75; 30 H	C_6H_5	t (7.68)	7.44; 2 H
C_6H_5	m	7.27–7.31; 2 H		d (7.72)	8.76; 2 H
	t (7.70)	7.35; 2 H		d (8.20)	8.87; 2 H
		$Cp^*_2Zr(OC(t\text{-}Bu){=}NC(t\text{-}Bu){=}N$ (**4b**)			
$C(CH_3)_3$	s	1.42; 9 H	$\eta^5\text{-}C_5(CH_3)_5$	s	1.74; 30 H
$C(CH_3)_3$	s	1.50; 9 H			
		$Cp^*_2Zr(OC(Me){=}C(Ph))$ (**5d**)			
$\eta^5\text{-}C_5(CH_3)_5$	s	1.78; 30 H	$C{=}C(C_6H_5)$	t (7.30)	7.04; 1 H
$C{=}C(CH_3)$	s	2.33; 3 H		d (8.29)	7.14; 2 H
				t (7.75)	7.35; 2 H
		$Cp^*_2Zr(OH)(OSO_2CF_3)$ (**7**)			
$\eta^5\text{-}C_5(CH_3)_5$	s	1.74; 30 H	*OH*	s	6.20; 1 H
		$Cp^*_2Zr(I)(CH_2C(CH_3)3)$ (**8**)			
CH_2	s	0.17; 2 H	$\eta^5\text{-}C_5(CH_3)_5$	s	1.87; 30 H
$C(CH_3)_3$	s	1.27; 9 H			
		$(\eta^5\text{-}C_5(CH_3)_5)(\eta^5{:}\eta^1\text{-}C_5(CH_3)_4CH_2)ZrI$ (**9**)			
$\eta^5\text{-}C_5(CH_3)_5$	s	1.87; 15 H	$C_5(CH_3)_4CH_2$	s	2.21; 3 H
$C_5(CH_3)_4CH_2$	s	1.33; 3 H	$C_5(CH_3)_4CH_2$	d (6.31)	1.56; 1 H
	s	1.55; 3 H		d (6.05)	2.28; 1 H
	s	1.95; 3 H			
		$Cp^*_2Zr(SH)(I)$ (**10**)			
$\eta^5\text{-}C_5(CH_3)_5$	s	1.89; 30 H	*SH*	s	2.69; 1 H
		$Cp^*_2Zr(S)(NC_5H_5)$ (**11a**)			
$\eta^5\text{-}C_5(CH_3)_5$	s	1.93; 30 H	NC_5H_5	t (7.63)	6.65; 1 H
NC_5H_5	t (6.54)	6.23; 1 H		d (5.51)	7.24; 1 H
	t (6.78)	6.33; 1 H		d (5.68)	9.45; 1 H
		$Cp^*_2Zr(S)(p\text{-}NC_5H_4C(CH_3)_3)$ (**11b**)			
$\eta^5\text{-}C_5(CH_3)_5$	1.2	1.98; 30 H	$p\text{-}NC_5H_4C(CH_3)_3$	dd (5.96, 2.22)	6.65; 1 H
$p\text{-}NC_5H_4C(CH_3)_3$	s	0.85; 9 H		dd (6.03)	7.29; 1 H
$p\text{-}NC_5H_4C(CH_3)_3$	dd (6.04, 2.12)	6.41; 1 H		d (6.08)	9.39; 1 H
		$Cp^*_2Zr(SC(Ph){=}NC(Ph){=}N)$ (**12**)			
$\eta^5\text{-}C_5(CH_3)_5$	s	1.75; 30 H	C_6H_5	t (7.61)	7.38; 2 H
C_6H_5	m	7.20–7.27; 2 H		d (8.31)	8.67; 2 H
	t (7.39)	7.30; 2 H		d (8.40)	8.91; 2 H
	t (7.39)	7.30; 2 H			
		$Cp^*_2Zr(SC(Et){=}C(Et))$ (**13a**)			
$\eta^5\text{-}C_5(CH_3)_5$	s	1.79; 30 H	$C{=}CCH_2CH_3$	t (7.42)	1.42; 3 H
$C{=}CCH_2CH_3$	t (7.54)	1.11; 3 H	$C{=}CCH_2CH_3$	m	2.52–2.61; 4 H
		$Cp^*_2Zr(SC(Ph){=}C(Ph))$ (**13b**)			
$\eta^5\text{-}C_5(CH_3)_5$	s	1.81; 30 H	$C{=}CC_6H_5$	t (7.81)	7.05; 2 H
$C{=}CC_6H_5$	m	6.84–6.87; 3 H		t (7.66)	7.12; 2 H
	t (7.36)	7.00; 1 H		d (8.17)	7.78; 2 H
		$Cp^*_2Zr(SC(p\text{-}tolyl){=}C(p\text{-}tolyl))$ (**13c**)			
$\eta^5\text{-}C_5(CH_3)_5$	s	1.85; 30 H	$C{=}CC_6H_4CH_3$	m	6.81–6.89; 4 H
$C{=}CC_6H_4CH_3$	s	2.09; 3 H		d (7.94)	6.98; 2 H
	s	2.11; 3 H		d (8.02)	7.74; 2 H
		$(Cp^*_2(SH)Zr)_2(\mu\text{-}S)$ (**14**)			
$\eta^5\text{-}C_5(CH_3)_5$	s	1.98; 30 H	*SH*	s	1.34; 2 H
	s	1.93; 30 H			

[a] Solvent used was benzene-d_6 in all cases, except for THF-d_8 in the case of **3**.

Table VI. $^{13}C\{^1H\}$ NMR Spectroscopic Data[a]

assignt	δ, ppm	assignt	δ, ppm
$Cp^*_2Zr(OC(o\text{-}C_6H_4)=C(Ph)(H))$ (2a)			
ipso	196.03	phenyl *C*H	126.16
	163.60		125.37
	156.66		123.61
	140.72	$\eta^5\text{-}C_5(CH_3)_5$	121.88
phenyl *C*H	136.75	vinyl *C*H	99.05
	128.29	$\eta^5\text{-}C_5(CH_3)_5$	11.20
	128.08		
$Cp^*_2Zr(OC(o\text{-}C_6H_4CH_3)=C(Tol)(H))$ (2b)			
ipso	195.42	*p*-tolyl *C*H	127.90
	162.49		126.35
	153.87		123.29
	137.75	$\eta^5\text{-}C_5(CH_3)_5$	121.05
	134.19	vinyl *C*H	98.64
	132.52	*p*-tolyl CH_3	21.61
p-tolyl *C*H	136.72		21.29
	129.03	$\eta^5\text{-}C_5(CH_3)_5$	11.03
$(\eta^5\text{-}C_5(CH_3)_5)Zr(OC(Ph)=C(H)C(Ph)(\eta^5\text{-}C_5(CH_3)_4CH_2$ (3)			
ipso	197.07	$\eta^5\text{-}C_5(CH_3)_4CH_2$	126.12
	160.11		123.16
	151.70		122.38
	141.61		109.45
	140.17	$\eta^5\text{-}C_5(CH_3)_5$	119.56
phenyl *C*H	128.65	vinyl *C*H	113.85
	128.03	$(\eta^5\text{-}C_5(CH_3)_4CH_2$	34.65
	127.70	$(\eta^5\text{-}C_5(CH_3)_4CH_2$	12.86
	126.89		11.17
	126.15		10.09
	125.37		9.94
$\eta^5\text{-}C_5(CH_3)_4CH_2$	130.75	$\eta^5\text{-}C_5(CH_3)_5$	11.29
$Cp^*_2Zr(OC(Ph)=NC(Ph)=N)$ (4a)			
ipso	164.88	aromatic	129.48
	158.96		129.43
	141.46		128.44
	139.77		128.29
aromatic	130.95	$\eta^5\text{-}C_5(CH_3)_5$	120.94
	129.90	$\eta^5\text{-}C_5(CH_3)_5$	11.15
$Cp^*_2Zr(OC(t\text{-}Bu)=NC(t\text{-}Bu)=N)$ (4b)			
ipso	176.79	$C(CH_3)_3$	39.49
	172.01	$C(CH_3)_3$	29.89
$\eta^5\text{-}C_5(CH_3)_5$	119.27		28.92
$C(CH_3)_3$	40.03	$\eta^5\text{-}C_5(CH_3)_5$	11.04
$Cp^*_2Zr(OC(Me)=C(Ph))$ (5d)			
ipso	156.09	aromatic	122.22
ipso	144.37	$\eta^5\text{-}C_5(CH_3)_5$	119.75
ipso	137.60	$C=C(CH_3)$	19.12
aromatic	129.16	$\eta^5\text{-}C_5(CH_3)_5$	11.18
	128.16		
$Cp^*_2Zr(OH)(OSO_2CF_3)$ (7)			
$\eta^5\text{-}C_5(CH_3)_5$	11.27	CF_3	120.42
$\eta^5\text{-}C_5(CH_3)_5$	123.05		
$Cp^*_2Zr(I)(CH_2C(CH_3)_3)$ (8)			
$\eta^5\text{-}C_5(CH_3)_5$	121.78	$C(CH_3)_3$	35.77
CH_2	69.91	$\eta^5\text{-}C_5(CH_3)_5$	13.52
$C(CH_3)_3$	36.17		
$(\eta^5\text{-}C_5(CH_3)_5)(\eta^5\text{:}\eta^1\text{-}C_5(CH_3)_4CH_2)ZrI$ (9)			
$\eta^5\text{:}\eta^1\text{-}C_5(CH_3)_4CH_2$	128.94	$\eta^5\text{:}\eta^1\text{-}C_5(CH_3)_4CH_2$	70.44
	128.10	$\eta^5\text{:}\eta^1\text{-}C_5(CH_3)_4CH_2$	18.57
	121.68		13.36
	121.61		12.98
	118.66		10.31
$\eta^5\text{-}C_5(CH_3)_5$	120.12	$\eta^5\text{-}C_5(CH_3)_5$	11.24
$Cp^*_2Zr(SH)(I)$ (10)			
$\eta^5\text{-}C_5(CH_3)_5$	121.88	$\eta^5\text{-}C_5(CH_3)_5$	13.40
$Cp^*_2Zr(S)(NC_5H_5)$ (11a)			
NC_5H_5	161.99	NC_5H_5	122.17
	148.27	$\eta^5\text{-}C_5(CH_3)_5$	118.60
	137.37	$\eta^5\text{-}C_5(CH_3)_5$	12.69
	124.09		
$Cp^*_2Zr(S)(p\text{-}NC_5H_4CH_3)$ (11b)			
$p\text{-}NC_5H_C(CH_3)_3$	162.38, ipso	$\eta^5\text{-}C_5(CH_3)_5$	118.54
	162.18	$p\text{-}NC_5H_4C(CH_3)_3$	34.63
	148.25	$p\text{-}NC_5H_4C(CH_3)_3$	29.81
	121.29	$\eta^5\text{-}C_5(CH_3)_5$	12.74
	119.54		
$Cp^*_2Zr(SC(Ph)=NC(Ph)=N)$ (12)			
ipso	172.69	$C=C(C_6H_5)$	130.02
	160.79		129.06
	145.18		128.54
	139.27		127.96
$C=C(C_6H_5)$	130.28	$\eta^5\text{-}C_5(CH_3)_5$	119.01
	130.13	$\eta^5\text{-}C_5(CH_3)_5$	11.52
$Cp^*_2Zr(SC(Et)=C(Et))$ (13a)			
$C=CCH_2CH_3$	186.56	$C=CCH_2CH_3$	25.94
	115.34	$C=CCH_2CH_3$	16.12
	118.69		15.52
$\eta^5\text{-}C_5(CH_3)_5$	118.69	$\eta^5\text{-}C_5(CH_3)_5$	11.79
$C=CCH_2CH_3$	27.50		
$Cp^*_2Zr(SC(Ph)=C(Ph))$ (13b)			
aromatic	185.58	aromatic	128.46
	118.60		127.78
ipso	142.45		126.66
ipso	140.99		123.66
aromatic	130.56	$\eta^5\text{-}C_5(CH_3)_5$	118.60
	130.49	$\eta^5\text{-}C_5(CH_3)_5$	11.93
$Cp^*_2Zr(SC(p\text{-}tolyl)=C(p\text{-}tolyl))$ (13c)			
aromatic	185.23	aromatic	130.49
	117.26		129.24
ipso	139.70		128.53
	138.04, ipso	$\eta^5\text{-}C_5(CH_3)_5$	120.15
	135.92, ipso	$C=C(C_6H_4CH_3)$	21.11
	132.68, ipso		21.03
aromatic	130.59	$\eta^5\text{-}C_5(CH_3)_5$	11.97
$(Cp^*_2(SH)Zr)_2(\mu\text{-}S)$ (14)			
$\eta^5\text{-}C_5(CH_3)_5$	120.81	$\eta^5\text{-}C_5(CH_3)_5$	13.00
	120.04		12.71

[a] Solvent used was benzene-d_6 in all cases, except for THF-d_8 in the case of **2a** and **4a**.

features or trends. The largest peak in the final difference Fourier map had an electron density of 0.32 e/Å^3, and the lowest excursion was −0.24 e/Å^3. There was no indication of secondary extinction in the high-intensity, low-angle data, except for the two reflections noted above.

For this compound and all others in this paper that were studied by X-ray diffraction, full details were included as supplementary data with the preliminary communications of this work.[9] This material is provided with the archival edition of the journal, available in many libraries; alternatively, ordering information is given on any current masthead page.

Synthesis of $Cp^*_2Zr(OC(o\text{-}C_6H_3CH_3)=C(Tol)(H))$ (2b). A Pyrex bomb was charged with 1 (218 mg, 0.478 mmol) and di-*p*-tolylacetylene (350 mg, 1.70 mmol) in 25 mL of benzene and the mixture thoroughly degassed. The bomb was fully immersed in an oil bath and heated at 160 °C for 24 h. The orange solution was filtered and taken to dryness in vacuo. The residue was transferred to a sublimation apparatus, where the excess di-*p*-tolylacetylene was sublimed onto a cold finger under vacuum at 100 °C for 4 h. The remaining orange solid was washed with cold hexane (5 mL) and dried in vacuo, affording 217 mg (78%) of pure material: IR (C_6H_6) 2910, 1596, 1509, 1441, 1380, 1344, 1142, 1077, 1026, 884, 830 cm^{-1}; MS (EI) *m/e* 582 (M^+), 119 (base). Anal. Calcd for $C_{36}H_{44}OZr$: C, 74.04; H, 7.59. Found: C, 74.25; H, 7.72.

Synthesis of $(\eta^5\text{-}C_5(CH_3)_5)Zr(OC(Ph)=C(H)C=C(Ph)(\eta^5\text{-}C_5(CH_3)_4CH_2))$ (3). $Cp^*_2Zr(Ph)(OH)$ (200 mg, 0.439 mmol) and 1,4-diphenyl-1,3-butadiyne (350 mg, 1.73 mmol) were dissolved in 25 mL of benzene; the mixture was placed in a Pyrex

bomb and freeze–pump degassed. This solution was heated at 160 °C for 24 h, filtered, and lyophilized. The remaining diyne was sublimed under vacuum onto a cold finger at 100 °C for 4 h, leaving a dark red solid. This solid was washed with 3 × 7 mL of cold hexane and dried in vacuo, yielding 224 mg (84%) of spectroscopically pure compound: IR (C_6H_6) 2959, 2907, 1595, 1459, 1443, 1431, 1378, 1319, 1272, 1071, 1022, 762, 696 cm^{-1}; MS (EI) m/e 578 (M^+), 202 (base). Anal. Calcd for $C_{36}H_{40}OZr$: C, 74.56; H, 6.95. Found: C, 73.72; H, 6.94. Despite several attempts, more satisfactory elemental analysis results could not be obtained on this material or on samples recrystallized from THF–hexane.

X-ray Structural Data for 3. Large columnar crystals of **3** were obtained by slow crystallization from THF–hexane. Fragments cleaved from some of these crystals were mounted, and X-ray data were collected as described above for complex **2a**. The final cell parameters and specific data collection parameters for this data set are given in Table I.[11]

The 4150 raw intensity data were treated as for **2a**. The data were corrected for a 3.0% reduction in the intensity standards. Inspection of the azimuthal scan data showed a variation I_{min}/I_{max} = ±1% for the average curve. No absorption correction was applied. Inspection of the systematic absences indicated uniquely space group $P2_1/n$. Removal of systematically absent and redundant data left 3882 unique data in the final data set. The structure was solved by Patterson methods and refined via standard least-squares and Fourier techniques as described above for **2a** (including treatment of the hydrogen atoms).

Least-squares analysis of the data, and correction for anomalous dispersion, were carried out as described for **2a**; the p factor was again set to 0.03. The final residuals for 343 variables refined against 3176 data for which $F^2 > 3\sigma(F^2)$ were R = 2.82%, R_w = 3.96%, and GOF = 1.99. The R value for all 3882 data was 4.13%.

Inspection of the residuals ordered in ranges of $(\sin\theta)/\lambda$, $|F_o|$, and parity and value of the individual indexes showed no unusual features or trends. The largest peaks in the final difference Fourier map had an electron density of ±0.22 e/Å^3. There was no indication of secondary extinction in the high-intensity, low-angle data.

Preparation of $Cp^*_2Zr(OC(Ph){=}NC(Ph){=}N)$ (4a). A Pyrex bomb was charged with 1 (300 mg, 0.658 mmol) and benzonitrile (350 mg, 3.39 mmol) in 30 mL of benzene and the mixture thoroughly degassed. The bomb was fully immersed in an oil bath and heated at 160 °C for 24 h. The orange solution was filtered and taken to dryness in vacuo. The residue was dissolved in a minimum of ether; this solution was filtered and cooled to −40 °C overnight. Yellow-orange crystals deposited and were washed with cold hexane, affording 74% of spectroscopically pure compound. Alternatively, this compound can be prepared in comparable yield as described below for **4b** using ca. 4 equiv of benzonitrile: IR (C_6H_6) 2980, 1599, 1567, 1467, 1439, 1379, 1315, 1293, 1242, 1014, 722, 703 cm^{-1}; MS (EI) m/e 582 (M^+), 103 (base). Repeated analysis of this and recrystallized samples did not give completely satisfactory results. Anal. Calcd for $C_{34}H_{40}N_2OZr$: C, 69.94; H, 6.90; N, 4.80. Found: C, 69.32; H, 6.92; N, 4.71.

X-ray Structural Data for 4a. Large yellow rodlike crystals of **4a**·0.5C_7H_8 were obtained by slow crystallization from toluene–hexane at −40 °C. Some of these crystals were mounted, and X-ray data were collected as described above for complex **2a**. The final cell parameters and specific data collection parameters for this data set are given in Table I.[11]

The 4855 raw intensity data were treated as for **2a**. No correction for crystal decomposition was necessary. Inspection of the azimuthal scan data showed the variation I_{min}/I_{max} = 0.93 for the average curve. An empirical absorption correction based on the observed variation was applied to the data. Inspection of the systematic absences indicated uniquely space group $P2_1/c$. Removal of systematically absent and redundant data left 4337 unique data in the final data set. The structure was solved by Patterson methods and refined via standard least-squares and Fourier techniques as described above for **2a** and **3** (including treatment of the hydrogen atoms). A number of large peaks near the inversion center at $^1/_2$, $^1/_2$, 0 were interpreted as a disordered toluene of solvation. Evidence of disorder of the oxygen and the nitrogen atoms of the metallacycle based on the distances and thermal parameters was confirmed by a reduction in the residuals when both positions were refined with a scattering factor that was the average of those of nitrogen and oxygen. Three reflections were removed from the data set for abnormally poor agreement between F_{obs} and F_{calc}.

Least-squares analysis of the data and correction for anomalous dispersion were carried out as described for **2a**; the p factor was again set to 0.03. The final residuals for 389 variables refined against 3598 data for which $F^2 > 3\sigma(F^2)$ were R = 3.13%, R_w = 4.25%, and GOF = 2.09. The R value for all 4337 data was 4.28%. In the final cycles of refinement a secondary extinction parameter was included (maximum correction 11% on F). The larget peak in the final difference Fourier map had an electron density of −0.32 e/Å^3, and the lowest excursion was −0.34 e/Å^3. Both were located near the Zr atom.

Synthesis of $Cp^*_2Zr(OC(t\text{-}Bu){=}NC(t\text{-}Bu){=}N)$ (4b). $Cp^*_2Zr(OH)(OSO_2CF_3)$ was generated in situ by suspending $Cp^*_2Zr(OH)(Cl)$ (100 mg, 0.241 mmol) and $AgOSO_2CF_3$ (65 mg, 0.25 mmol) in 10 mL of benzene in a vial and stirring at room temperature for 0.5 h. The resulting peach-colored suspension was filtered to remove AgCl. The clear filtrate was treated with 95 mg (1.14 mmol) of trimethylacetonitrile and 51 mg (0.256 mmol) of $KN(Si(CH_3)_3)_2$ with stirring. An off-white precipitate formed almost immediately, and stirring was continued overnight with the gradual formation of a yellow suspension. This suspension was filtered and freeze-dried. The yellow solid was dissolved in a minimum of benzene, layered with hexane, and let stand for 2 days. Large pale yellow crystals formed and were collected and dried (105 mg, 80%): IR (C_6H_6) 2955, 2907, 2861, 1604, 1380, 1357, 1294, 1230, 1204, 1094, 874 cm^{-1}; MS (EI) m/e 542 (M^+), 42 (base). A completely satisfactory elemental analysis could not be obtained; our best result was as follows. Anal. Calcd for $C_{30}H_{48}N_2OZr$: C, 66.24; H, 8.89; N, 5.15. Found: C, 65.60; H, 9.22; N, 4.78.

Preparation of $Cp^*_2Zr(OSO_2CF_3)(OH)$ (7). In a typical preparation, $Cp^*_2Zr(OH)(Cl)$ (220 mg, 0.53 mmol) and $AgOSO_2CF_3$ (143 mg, 0.56 mmol) were suspended in 15 mL of benzene and stirred at room temperature for 0.5 h. A peach-colored precipitate (presumably AgCl) formed and was removed by filtration. The clear filtrate was taken to dryness in vacuo; the residue was washed several times (5 × 2 mL) with hexane and the solvent removed in vacuo. This procedure produced analytically pure material (240 mg) in 86% yield: ^{19}F NMR (C_6D_6) −76.12 ppm, referenced to an external Freon standard; IR (C_6H_6) 3650, 2865, 1383, 1346, 1236, 1185, 1001, 634 cm^{-1}. Anal. Calcd for $C_{21}H_{31}SO_4F_3Zr$: C, 47.79; H, 5.92. Found: C, 47.59; H, 5.84.

Preparation of $Cp^*_2Zr(OC(Ph){=}C(Ph))$ (5a). $Cp^*_2Zr(OH)(OSO_2CF_3)$ was generated in situ by the reaction of 200 mg (0.483 mmol) of $Cp^*_2Zr(OH)Cl$ and 130 mg (0.507 mmol) of $AgOSO_2CF_3$ in 15 mL of benzene. Filtration of this solution was followed by the addition of 300 mg (1.68 mmol) of diphenylacetylene and 100 mg (0.50 mmol) of $KN(Si(CH_3)_3)_2$ with stirring. A white precipitate formed nearly immediately and was slowly (over several hours) replaced by the deep red color of the metallacyclobutene. Stirring was continued for 18 h, and the solution was filtered and freeze-dried. The deep red solid was placed in a sublimation apparatus and heated at 50 °C for 4 h to remove excess diphenylacetylene. The remaining solid was redissolved in a minimum of pentane and the solution slowly cooled to −40 °C, resulting in the formation of 86 mg (32%) of crystalline material. It was found to be spectroscopically identical (^1H NMR) to that reported by Hillhouse.[15]

Preparation of $Cp^*_2Zr(OC(Me){=}C(Ph))$ (5d). $Cp^*_2Zr(OH)(Cl)$ (500 mg, 1.21 mmol) and $AgOSO_2CF_3$ (325 mg, 1.26 mmol) were suspended in 25 mL of benzene and stirred at room temperature for 0.5 h. The peach-colored suspension was filtered to remove AgCl. The clear filtrate was treated with 560 mg (4.8 mmol) of 1-phenyl-1-propyne and 245 mg (1.23 mmol) of $KN(Si(CH_3)_3)_2$ with stirring. An off-white precipitate formed almost immediately, and stirring was continued overnight with the gradual formation of a red solution. The solution was filtered and freeze-dried. The red solid was redissolved in a minimum of pentane and the solution cooled slowly to −40 °C. After 2 days large red blocks had formed; these were collected, washed with 1 mL of cold hexane, and dried in vacuo, yielding 252 mg (42%) of compound: IR (C_6H_6) 2907, 2863, 1616, 1589, 1380, 1346, 1237, 1200, 1182, 1001, 633 cm^{-1}; MS (EI) m/e 492 (M^+), 115 (base). Anal. Calcd for $C_{29}H_{38}OZr$: C, 70.53; H, 7.76. Found: C, 69.52; H, 7.88. Repeated analyses of recrystallized samples were con-

sistently low in carbon content.

Synthesis of $Cp^*_2Zr(CH_2C(CH_3)_3)(I)$ (8). $Cp^*_2ZrI_2$ (2.85 g, 4.63 mmol) was suspended in 50 mL of benzene and the mixture treated with 0.377 g (4.64 mmol) of neopentyllithium. This solution was stirred overnight, and solvent was removed in vacuo. The orange-yellow residue was dissolved in hexane and the solution filtered to remove LiI. This solution was taken to dryness and the residue washed with 5 mL of cold hexane to yield 2.34 g (90%) of pure material: IR (C_6H_6) 2942, 2903, 2727, 1380, 1357, 1225, 1200, 1178 cm^{-1}. Anal. Calcd for $C_{25}H_{41}IZr$: C, 53.65; H, 7.38. Found: C, 53.46; H, 7.40.

Preparation of $(\eta^5\text{-}C_5(CH_3)_5)(\eta^5{:}\eta^1\text{-}C_5(CH_3)_4CH_2)ZrI$ (9). A Pyrex bomb was charged with 994 mg (1.78 mmol) of **8** and 30 mL of benzene and was thoroughly degassed. This solution was thermolyzed at 140 °C for 4 h, during which time the solution changed from orange-yellow to deep red-purple. The benzene solution was fitlered and taken to dryness in vacuo. The deep purple residue was redissolved in ether and the solution filtered and reduced in volume (to ca. 5 mL). Cooling to −40 °C overnight resulted in the deposition of 703 mg (81%) of **9**: IR (C_6H_6) 2954, 2908, 2858, 1468, 1380, 1236, 1183, 1027 cm^{-1}; MS (EI) *m/e* 486 (M^+), 119 (base). Anal. Calcd for $C_{20}H_{29}IZr$: C, 49.27; H, 6.00. Found: C, 49.22; H, 6.03.

Synthesis of $Cp^*_2Zr(SH)(I)$ (10). In a typical preparation, 1.00 g (2.05 mmol) of **9** was dissolved in 25 mL of benzene and placed in a Pyrex bomb, which was cooled to −196 °C and evacuated. H_2S (1.2 equiv) was condensed into the bomb via a known volume bulb, and the bomb was closed off and warmed to room temperature. The purple color of **9** immediately changed to yellow upon thawing. This solution was filtered, and the benzene was removed in vacuo. The yellow residue was redissolved in ether, the solution was filtered, and solvent was removed to the point of incipient crystallization. The flask was placed in a −40 °C freezer overnight, and the yellow crystals (0.91 g, 85%) that formed were collected and dried in vacuo: IR (C_6H_6) 2985, 2953, 2906, 1451, 1426, 1380, 1237, 1182, 1022 cm^{-1}. Once again, repeated attempts at analysis gave unsatisfactory results; an example is as follows. Anal. Calcd for $C_{20}H_{31}ZrSI$: C, 46.05; H, 5.99. Found: C, 46.53; H, 6.16.

Preparation of $Cp^*_2Zr(S)(NC_5H_5)$ (11a). Typically, 300 mg (0.575 mmol) of **10** was dissolved in 25 mL of benzene and the solution treated sequentially with 180 mg (2.3 mmol) of pyridine and 117 mg (0.585 mmol) of $KN(Si(CH_3)_3)_2$. Stirring was continued overnight, and the resulting orange suspension was filtered and the solid remaining (mainly KI) was washed with benzene until the washings were colorless. This benzene solution was taken to dryness in vacuo, and the residue was redissolved in a minimum amount of benzene and the solution layered with hexane. Orange needles (222 mg, 82%) deposited over several days: IR (Nujol) 1600, 1212, 1069, 1021, 755, 706 cm^{-1}. Anal. Calcd for $C_{25}H_{35}SNZr$: C, 63.50; H, 7.46; N, 2.96. Found: C, 63.00; H, 7.29; N, 2.90.

Synthesis of $Cp^*_2Zr(S)(4\text{-}t\text{-}Bu\text{-}C_5H_4N)$ (11b). In a manner similar to the preparation of **11a** above, 100 mg (0.192 mmol) of **10** was dissolved in 10 mL of benzene and the solution treated sequentially with 70 mg (0.52 mmol) of 4-*tert*-butylpyridine and 40 mg (0.20 mmol) of $KN(Si(CH_3)_3)_2$. A light yellow solid formed nearly immediately, and stirring was continued for 8 h, resulting in the generation of a red-orange solution and an off-white precipitate. This solution was filtered to remove KI and taken to dryness. Dissolution in a minimum of benzene and layering with hexane resulted in 73 mg (72%) of orange crystals after several days. Crystals suitable for an X-ray diffraction study were obtained in this manner: IR (Nujol) 1614, 1224, 1064, 1021, 838, 723 cm^{-1}. Anal. Calcd for $C_{29}H_{43}NSZr$: C, 65.85; H, 8.19; N, 2.64. Found: C, 65.41; H, 8.30; N, 2.35.

X-ray Structural Data for 11b. Large yellow-orange crystals were obtained by layering hexane on top of a saturated benzene solution of **9a**. Fragments cleaved from some of these crystals were mounted and X-ray data collected as described above for **2a**, **3**, and **4**. The crystals were cooled to 191 K by a cold nitrogen flow apparatus previously calibrated by a thermocouple at the sample position. The final cell parameters and specific data collection parameters for this data set are given in Table I.[11]

A total of 4292 raw intensity data were collected and analyzed as described for the structures above. Intensities of three check reflections showed ca. 8.5% decrease (linear) over the course of the experiment; the data were corrected for this decrease. Inspection of the azimuthal scan data showed the variation I_{min}/I_{max} = ±6% for the average curve. An empirical absorption correction was applied on the basis of this observed variation. Inspection of the systematic absences indicated uniquely space group $P2_1/c$. Removal of systematically absent and redundant data left 3669 unique data in the final data set.

The zirconium atom was located from a Patterson map; all remaining non-hydrogen atoms were found by Fourier maps and refined via standard least-squares techniques. All non-hydrogen atoms were refined anisotropically and handled as summarized earlier; the *p* factor, analytical forms of the scattering factors, and corrections for anomalous dispersion were also handled as described above. The final residuals for 289 variables refined against 2572 data for which $F^2 > 3.5\sigma(F^2)$ were R = 6.58%, R_w = 8.45%, and GOF = 3.33. The R value for all 3669 data was 6.58%. The largest peak in the final difference Fourier map had an electron density of 0.79 e/Å^3, and the lowest excursion was −0.53 e/Å^3. There was no indication of secondary extinction in the high-intensity, low-angle data.

Synthesis of $Cp^*_2Zr(SC(Ph){=}NC(Ph){=}N)$ (12). Compound **10** (100 mg, 0.192 mmol) and benzonitrile (80 mg, 0.78 mmol) were dissolved in 20 mL of benzene and the solution treated with 40 mg (0.20 mmol) of $KN(Si(CH_3)_3)_2$. The resulting suspension was stirred for 8 h, during which time it slowly turned yellow-orange. This solution was filtered and taken to dryness. Dissolution in benzene (ca. 10 mL) and addition of 20 mL of hexane precipitated 91 mg (79%) of orange-yellow crystals: IR (C_6H_6) 2906, 1609, 1575, 1438, 1378, 1237, 936, 770, 599 cm^{-1}. Anal. Calcd for $C_{34}H_{40}SN_2Zr$: C, 68.06; H, 6.72; N, 4.67. Found: C, 67.70; H, 6.67; N, 4.63.

Preparation of $Cp^*_2Zr(SC(Et){=}C(Et))$ (13a). This metallacycle is most easily prepared directly from **10** as follows. Complex **10** (335 mg, 0.642 mmol) and 200 mg (2.4 mmol) of 3-hexyne were dissolved in 30 mL of benzene in a vial. Potassium hexamethyldisilazide (141 mg, 0.706 mmol) was added, and the suspension was stirred overnight. Filtration of the red-orange solution and subsequent lyophilization yielded a red-orange solid. This solid was redissolved in a minimum of ether and the solution cooled to −40 °C, yielding 105 mg (35%) of spectroscopically pure compound: IR (C_6H_6) 2961, 2914, 2868, 1438, 1377, 1302, 1193, 1068 cm^{-1}. Anal. Calcd for $C_{26}H_{40}SZr$: C, 65.62; H, 8.47. Found: C, 64.92, 66.16; H, 8.49, 8.57. Repeated elemental analyses were consistently low in carbon content.

Synthesis of $Cp^*_2Zr(SC(Ph){=}C(Ph))$ (13b). Terminal sulfido complex **11a** (100 mg, 0.21 mmol) was dissolved in 20 mL of benzene; this solution was treated with 100 mg (0.56 mmol) of diphenylacetylene and placed in a Pyrex bomb. After the bomb was freeze–pump degassed, the solution was heated at 85 °C for 12 h, during which time the solution color changed from orange to deep red. After the solution was taken to dryness, diphenylacetylene was removed by sublimation (85 °C, 3 h under vacuum) onto a cold finger. The red-orange residue was redissolved in a minimum of benzene, filtered, and layered with hexane. A light red solid (55 mg, 45%) deposited over several days and was pure by ^1H NMR spectrometry: IR (C_6H_6) 2906, 1588, 1440, 1378, 1227, 1178, 937, 769 cm^{-1}. Anal. Calcd for $C_{34}H_{40}SZr$: C, 71.40; H, 7.05. Found: C, 70.83; H, 7.14. Repeated analyses on recrystallized samples were likewise low in carbon content.

X-ray Structural Data for 13b. Large red blocklike crystals were obtained by layering hexane onto a benzene solution of **13b**. Fragments cleaved from some of these crystals were mounted, and X-ray data were collected at low temperature as described for **11b**. The final cell parameters and specific data collection parameters for this data set are given in Table I.[11]

A total of 4165 raw intensity data were collected and analyzed as described above. Inspection of the intensity standards revealed a 0.2% reduction of the original intensity. The data were not corrected for this minute decay. Inspection of the azimuthal scan data showed the variation I_{min}/I_{max} = ±2% for the average curve. An empirical absorption correction was applied. Inspection of the systematic absences indicated either orthorhombic space group $Pna2_1$ or *Pnam*. Simple Wilson statistics favored the noncentrosymmetric space group $Pna2_1$. Successful solution and refinement in the acentric space gorup indicated that this was the correct choice. Removal of systematically absent and redundant

data left 1983 unique data in the final data set.

The zirconium and sulfur atoms were located from a Patterson map: all remaining non-hydrogen atoms were obtained from Fourier maps. The data were refined as described for the structures discussed above. All non-hydrogen atoms were handled as described earlier. Final refinement of this solution yielded an R value of 2.33% (R_w = 2.98%). Generation of the other enantiomorph and subsequent refinement converged to an R value of 2.26%, indicating that the second choice of polarity was correct.

The final residuals for 324 variables refined against 1773 data for which $F^2 > 3\sigma(F^2)$ were R = 2.26%, R_w = 2.89%, and GOF = 1.17. The R value for all 1983 data was 2.77%. The quantity minimized by the least-squares program, p factor, and corrections for anomalous dispersion were also handled as described above. The largest peaks in the final difference Fourier map had an electron density of ±0.23 e/Å^3. There was no indication of secondary extinction in the high-intensity, low-angle data.

Synthesis of $Cp^*_2Zr(SC(p\text{-}C_6H_4CH_3)=C(p\text{-}C_6H_4CH_3))$ (13c). As in the preparation of **13b**, a benzene solution of complex **11a** (100 mg, 0.21 mmol) and 130 mg (0.63 mmol) of di-*p*-tolylacetylene was thermolyzed in a degassed Pyrex bomb at 85 °C for 12 h. Excess alkyne was removed by sublimation at 85 °C onto a cold finger (under vacuum). Extraction of the red-orange residue into a minimum of benzene, filtration, and layering with hexane yielded 83 mg (65%) of microcrystalline material: IR (C_6H_6) 2907, 2888, 1518, 1248, 1178, 672 cm^{-1}. Anal. Calcd for $C_{36}H_{44}SZr$: C, 72.06; H, 7.39. Found: C, 71.62; H, 7.46.

Preparation of $(Cp^*_2(SH)Zr)_2(\mu\text{-}S)$ (14). $Cp^*_2ZrPh_2$ (500 mg, 0.97 mmol) was dissolved in 30 mL of toluene and the solution placed in a Pyrex bomb, frozen in liquid nitrogen, and thoroughly degassed. H_2S (1.50 equiv) was condensed into the bomb via a known volume bulb, and this mixture was thawed and heated at 80 °C for 12 h. The resulting yellow reaction mixture was filtered and taken to dryness in vacuo and the residue washed with 10 mL of ether, yielding 252 mg (63%) of bright yellow solid: IR (C_6H_6) 2951, 2906, 1378, 1248, 1178, 673 cm^{-1}. Anal. Calcd for $C_{40}H_{62}S_3Zr_2$: C, 58.48; H, 7.61; S, 11.71. Found: C, 58.42; H, 7.67; S, 11.49.

Acknowledgment. We thank the National Institutes of Health (Grant No. GM-25457) for financial support of this work, and M.J.C. gratefully acknowledges a postdoctoral (NRSA) fellowship from the NIH. We also thank Prof. G. L. Hillhouse for providing us with a sample of compound **5a**.

(Diphenylphosphino)methyl Complexes of Titanium and Zirconium: Synthesis and Characterization. Molecular Structure of $CpCp^*Ti(CH_2PPh_2)_2$ ($Cp = C_5H_5$; $Cp^* = C_5Me_5$)

Tomàs Cuenca, J. Carlos Flores, and Pascual Royo*

Departamento de Quimica Inorgànica, Facultad de Ciencias, Universidad de Alcalà de Henares, Campus Universitario, E-28871 Alcala de Henares, Madrid, Spain

Anne-Marie Larsonneur, Robert Choukroun,* and Françoise Dahan

Laboratoire de Chimie de Coordination du CNRS, UPR 8241, liê par conventions à l'Université Paul Sabatier et à l'Institut National Polytechnique de Toulouse, 205 Route de Narbonne, 31077 Toulouse Cedex, France

Received July 30, 1991

The reaction of $[C_5(CH_3)_5](C_5H_5)MCl_2$ (M = Ti, Zr) with 2 equiv of $LiCH_2PPh_2$·TMEDA offers a convenient method for the preparation of the corresponding dialkyl derivatives $[C_5(CH_3)_5](C_5H_5)M(CH_2PPh_2)_2$ where M = Ti and Zr in 95–100% yield. However, when this reaction is carried out with 1 equiv of $LiCH_2PPh_2$·TMEDA in the same conditions, the chloro alkyl complex of titanium $[C_5(CH_3)_5](C_5H_5)TiCl(CH_2PPh_2)$ is formed, whereas a mixture of the starting material and the dialkyl derivative is obtained for zirconium. These new complexes have been characterized by ^1H, ^{13}C, and $^{31}P\{^1H\}$ NMR measurements and elemental analysis. The ^1H NMR spectra show a clear diastereotopic behavior for the methylene protons of the CH_2 groups. The molecular structure of $[C_5(CH_3)_5](C_5H_5)Ti(CH_2PPh_2)_2$ as determined by X-ray diffraction methods is reported. The complex crystallizes in the space group $P2_1/c$ (No. 14), a = 17.323 (2) Å, b = 12.549 (1) Å, c = 16.497 (2) Å, β = 103.71 (2)°, Z = 4. The geometry around the Ti atom is normal. A weak agostic interaction Ti···H(4) can be proposed to be present in the structure of the solid state of this compound.

Introduction

Many important industrial processes[1] have been devised by using cyclopentadienyltitanium and -zirconium derivatives. An interesting class of complexes is those containing remote phosphine ligands with a M–C–P framework in which a functionalized tertiary phosphine is present. They were initially prepared as precursors to access the heterodinuclear compounds formed by group 4 metals and mainly late-transition-metal centers.[2] These

(1) (a) Wilkinson, G.; Stone, F. G. A.; Abel, E. W. *Comprehensive Organometllic Chemistry*; Vol. 3. (b) Wailes, P. C.; Coutts, R. S. P.; Weigold, H. *Organometallic Chemistry of Titanium, Zirconium and Hafnium*; Academic Press: New York, 1974. (c) Cardin, D. J.; Lapert, M. F.; Raston, C. L. *Chemistry of Organo-Zirconium and Hafnium Compounds*; John Willey and Sons: New York, 1986.

(2) (a) Schore, N. E.; Hope, H. *J. Am. Chem. Soc.* **1980**, *102*, 4251. (b) Choukroun, R.; Dahan, F.; Gervais, D.; Rifai, C. *Organometallics* **1990**, *9*, 1982. (c) Etienne, M.; Choukroun, R.; Basso-Bert, M.; Dahan, F.; Gervais, D. *Nouv. J. Chim.* **1984**, *8–9*, 531. (d) Choukroun, R.; Gervais, D. *J. Chem. Soc., Chem. Commun.* **1982**, 1300.

0276-7333/92/2311-0777$03.00/0